NASA TN D-256

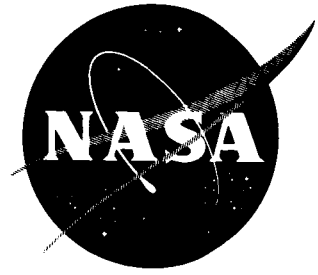

TECHNICAL NOTE

D-256

FATIGUE DAMAGE DURING COMPLEX STRESS HISTORIES

By H. W. Liu and H. T. Corten
University of Illinois

NATIONAL AERONAUTICS AND SPACE ADMINISTRATION
WASHINGTON

November 1959

NATIONAL AERONAUTICS AND SPACE ADMINISTRATION

TECHNICAL NOTE D-256

FATIGUE DAMAGE DURING COMPLEX STRESS HISTORIES

By H. W. Liu and H. T. Corten

SUMMARY

The influence of complex stress histories on the fatigue life of members has been investigated to determine the relation between the fatigue life and the relative number and amplitude of imposed cycles of stress. Stress history was taken into account in terms of the number of damage nuclei initiated by the highest applied stress and the propagation of damage by all subsequent cycles of stress. Wire specimens of three materials, 2024-T4 and 7075-T6 aluminum alloy and hard-drawn steel, were employed to provide a large number of inexpensive reproducible specimens. The data were statistically analyzed to obtain a measure of mean fatigue life of known reliability. Completely reversed two-stress repeated block experiments, the simplest form of complex stress history, were performed and analyzed to verify the hypothesis that the fatigue life was adequately described by a simple two-parameter expression involving (a) the percent of cycles at the high stress and (b) a stress interaction factor. The experimentally determined values of this stress interaction factor were correlated with the values of the high and low stress by a simple power relation.

The above relations were combined and extended to continuously varying stress-amplitude histories. For the one set of data completed, the agreement between the computed and experimentally determined fatigue life was excellent.

INTRODUCTION

In the design of limited-life members and structural components subjected to repeated loads, an accurate estimate of fatigue life is necessary. Current methods of estimating fatigue life frequently lead to either an overconservative or unsafe value. The common elements of this problem, (a) the random spectrum of loads, (b) the fatigue behavior of the components, generally known only for constant-amplitude loading, and (c) the influence of a complex load history on the fatigue behavior of the components, individually constitute complex problems. Adequate

design for limited-fatigue-life components will be achieved only as improved quantitative methods of analysis are developed for each phase of the problem.

This investigation studies the influence of complex stress histories on the fatigue behavior, specifically the fatigue life, of structural aluminum alloys and steels. It summarizes the results obtained during the early part of the program. A combined analytical and experimental investigation was undertaken in which the problem was subdivided into several simple phases. A hypothesis to describe the phenomena was introduced and experiments were devised to check this hypothesis. Based on the results of the several phases of this program, an analytical expression is presented for the fatigue life of a member under an arbitrary complex load history. In the present report, the experimental results are confined to the fatigue life of wire specimens subjected to two-stress repeated block loading and one condition of continuously varying load amplitude. Experiments were all conducted at room temperature employing completely reversed cycles of stress.

The first phase of the program consisted of determining the influence of the percent of cycles at the high stress on the fatigue life in the two-stress repeated block experiments. An hypothesis was formulated which lead to a simple analytical expression for fatigue life in terms of the percent of cycles at the high stress α and the stress interaction factor $R^{1/a}$, which depends only upon the high and low stresses, σ_1 and σ_2, respectively.

The second phase of the program consisted of investigating the interaction between the high and low stresses in the two-stress repeated block experiment. In this phase of the investigation, the high stress σ_1 was maintained constant and either six or seven different values of low stress were employed. Use of the values of the parameter $R^{1/a}$, determined previously, lead to a simple empirical correlation between $R^{1/a}$ and σ_1 and σ_2. Finally, the fatigue life for conditions where the stress amplitude varied in a continuous manner was investigated. One set of experimental results is included and compared with the fatigue life computed from the data obtained in the first two phases of the investigation.

The third phase of the investigation will consist of extending the study of the interaction of the high and low stresses employing a variety of high stresses as well as low stresses. Based on the analysis and results from all the two-stress repeated block experiments, the analytical expression for fatigue life for continuously varied amplitude experiments will be evaluated. The computed fatigue life will be compared with the fatigue life obtained experimentally for a wide variety of load histories.

In this investigation, wire specimens have been employed as a source of inexpensive reproducible specimens. In the analysis of results, the fatigue life from one load history was compared with fatigue life from another load history. Because of the statistical variability of fatigue life, the results of 20 specimens were obtained and statistically analyzed for nearly all experimental conditions. A measure of the average fatigue life was desired for comparison with the analytical results; therefore, a logarithmic-normal distribution of fatigue life was assumed. The experimental data are presented in terms of mean log N, standard deviation, and 95-percent confidence limits on the mean life.

Because all the results are analyzed by comparing the fatigue life of one set of wire specimens with that of another set, it is believed that the influence of specimen shape and fabrication was minimized. Further, it is anticipated that the analytical expressions developed and confirmed experimentally will be applicable to members of any size or shape. At the present time, the analytical expression for fatigue life under continuously varying load amplitude contains two parameters. The first parameter, α_i, is related to the number of load cycles in various stress intervals. The second parameter, $R_i^{1/a}$, is related primarily to the interaction at the various stress amplitudes and has been determined empirically. These two parameters correspond to the i^{th} stress level σ_i. From the results, it appears that the two-parameter expression is adequate to describe the variation of fatigue life for conditions of continuously varying load amplitude.

This investigation was conducted in the research laboratories of the Department of Theoretical and Applied Mechanics as part of the work of the Engineering Experiment Station, University of Illinois, under the sponsorship and with the financial assistance of the National Advisory Committee for Aeronautics. The advice and criticism of Professors G. M. Sinclair and T. J. Dolan is greatly appreciated. Acknowledgment is due to G. E. Mercer for his care in constructing the apparatus and to J. W. Melvin, C. H. Tang, and E. Mueller who assisted in various phases of this work.

SYMBOLS

a constant

B' constant

c radius of cross section of wire, in.

D	fatigue damage
D_f	damage at failure
d	constant
E	modulus of elasticity, psi
I	moment of inertia of cross section of specimen, in^4
K	constant
l	length of specimen, in.
M	bending moment
m	number of damage nuclei
N	number of cycles
N_g	fatigue life for complex stress histories
N_1	fatigue life at high stress
N_2	fatigue life at low stress
n	number of cycles in each repeated block
P	axial compressive force, lb
q	number of stress levels
$R^{1/a}$	stress interaction factor
r	coefficient of crack propagation
S_r	reduced stress
α	percent of cycles at high stress
β	reduction factor for crack propagation at σ_1 by strain aging
γ	exponent on cycle ratio, a constant for a given stress
Δ	maximum deflection of specimen
δ	fraction of cycles in each repeated block needed to break pinned dislocations
θ	angular deflection of specimen, deg

σ maximum alternating-stress amplitude, psi

σ_0 constant

σ_1 high stress

σ_2 low stress

ϕ cycle ratio

$\Delta\phi$ cycle ratio increment

Subscripts:

ac actual

ex experimental

f failure

th theoretical

1 conditions at low stress

2 conditions at high stress

MATERIALS AND APPARATUS

Materials

Wire specimens of three materials, 2024-T4 aluminum alloy, 7075-T6 aluminum alloy, and hard-drawn steel designated as "Brite Basic," were employed in this investigation to satisfy the requirement of inexpensive reproducible specimens. All three kinds of wire were tested in the "as-received" condition. The steel wire was straightened and cut into 3-foot lengths, and the aluminum wire was heat-treated following the drawing operation and also cut into 3-foot lengths by the manufacturer. The diameter of aluminum wire was 0.100 inch and the diameter of steel wire was 0.050 inch. The stress-strain curves for these three materials are shown in figure 1. The mechanical properties determined thereby are listed in the following table:

Wire specimen	Yield strength, psi		Ultimate strength, psi
	0.2-Percent offset	0.03-Percent offset	
2024-T4 Aluminum alloy	56,200	50,700	69,900
7075-T6 Aluminum alloy	69,000	62,700	80,000
Hard-drawn steel	108,000	93,500	130,000

Wire-Fatigue Testing Machines

The use of wire specimens required that the region of maximum stress was located away from the points where the specimen was gripped or loaded. A deflected rotating strut loaded with axial compressive forces met this requirement. The total stress in the specimen was composed of two components, bending and compressive stresses. However, the compressive stress was small and, therefore, the maximum alternating stress at the center of the specimen was given by the equation

$$\sigma = \frac{Mc}{I} = \frac{P\,\Delta c}{I} = \left(\frac{Pl^2}{EI}\right)\left(\frac{\Delta}{l}\right)\left(\frac{Ec}{l}\right) \tag{1}$$

where

c radius of cross section of wire, in.

E modulus of elasticity, psi

I moment of inertia of cross section of specimen, $in.^4$

l length of specimen, in.

P axial compressive force, lb

Δ maximum deflection of specimen, in.

σ maximum alternating-stress amplitude, psi

The quantities Pl^2/EI and Δ/l are dimensionless quantities related to the configuration of the deflected specimen (ref. 1).

The development of the machine used in this investigation was previously reported in detail (ref. 2). Briefly, one end of the specimen, a deflected rotating strut, was rigidly fixed, while the other end

followed an appropriately curved path such that, theoretically, both ends of the specimen were subjected to zero bending moment. The trace of this curved path is very closely approximated by a circular arc. In order to facilitate the fabrication of the machine, a circular arc was used instead of the theoretical curved path. The error introduced by the circular arc is shown in figure 2(a) where the difference in length of deflected specimen between theoretical and circular-arc track is plotted against the angular deflection of the specimen θ between the original undeflected position of the specimen and the line connecting the two ends of the deflected specimen. An approximate calculation of the stress in the specimen caused by the circular-arc approximation was made by assuming a sine wave for the configuration of the deflected specimen (ref. 2). The results of this approximation are shown by the broken line in figure 2(b). The nominal stress given by equation (1) is used in this report and is shown by the solid line in figure 2(b). The nominal stress was obtained by assuming the theoretical-curve path for the movable end of the specimen. The actual stress in the specimen is on a line between these two rather narrow limits. For any straight line between these limits in figure 2(b), the stress is related to the angle θ by the expression

$$\sigma = K\theta$$

where K is some constant. In this investigation, only a stress ratio σ_2/σ_1 is used in the analysis. Therefore, since both of these stresses are linear functions of θ, it is immaterial which value of stress is used in the analysis.

In figure 3(a) the wire machine is shown arranged to test specimens under two-stress repeated block loading. The stress history employed in this test is shown in figure 4(a). One end of the specimen, the drive end, was held rigidly by the chuck (A). The other end of the specimen was fitted into a miniature bearing which was attached to the movable trolley (B). The trolley was readily adjustable to any position along the circular track (CD). The chuck (A) was geared to the circular cam (E). As the cam turned, two pips on the cam activated the solenoid (F) through two microswitches (G) and changes the stress in the specimen by moving the trolley (B). The percent of the life of the specimen at high stress was varied by appropriate spacing of the two pips.

Figure 3(b) shows a specimen and machine arranged for the continuously varying stress amplitude experiments. A typical stress history is shown in figure 4(b). In this experiment, a curved cam (E) was employed to move the trolley (B) by means of the follower (H). The large cam made 1 revolution for each 10,000 revolutions of the specimen. Therefore, the stress history shown in figure 4(b) (also fig. 4(a)) was repeated every 10,000 cycles. The machines were run at

slightly different speeds to minimize vibration between 4,000 and 6,000 rpm.

This machine offered wide adaptability to various load patterns and, at the same time, offered economical means for compiling a large amount of data. However, considerable care was required in fabricating the machine and in running the experiments to obtain consistent reproducible data. Reproducibility of data was checked periodically by rerunning the constant stress-amplitude S-N experiments.

The number of cycles spent at the high stress was determined by the setting of pips on the large cam (E) and then independently checked by counting the number of revolutions at the high stress when the specimen was revolving slowly. Because the action of the solenoid was independent of the speed of the machine, the number of cycles consumed in moving from the low to the high stress and back again was determined at normal operating speed by taking high-speed motion pictures with a Wollensak Fastax camera. It was established that from 5 to 10 cycles were required to change from either the low to the high stress or from the high to the low stress.

ANALYSIS OF CUMULATIVE DAMAGE

Fatigue damage D was visualized as a joining or accumulation of cracks and was treated in terms of (a) the number of damage nuclei formed and (b) the rate of crack propagation. The following summary of experimental observations was used in formulating a quantitative expression for cumulative damage (ref. 3):

(1) A nucleation period (possibly a small number of cycles) may be required to initiate permanent fatigue damage.

(2) The number of damage nuclei (submicroscopic voids) that subsequently join to form a larger crack increases as the stress increases.

(3) Damage at a given stress amplitude propagates at rates that increase with numbers of cycles.

(4) The rate of propagation of damage per cycle increases as the stress increases.

(5) The total damage that constitutes failure in a given member is constant for all stress histories.

(6) Damage is propagated at stress levels that are lower than the minimum stress required to initiate damage.

The fatigue damage D caused by number of cycles of a particular stress amplitude was expressed as

$$D = mrN^a \tag{2}$$

where

a constant

m number of damage nuclei

N number of cycles

r coefficient of crack propagation

For constant stress amplitudes, σ_1 or σ_2, damage at failure D_f was expressed as

$$D_f = m_1 r_1 N_1^{a_1} = m_2 r_2 N_2^{a_2} \tag{3}$$

The progress of damage D is shown schematically in figure 5.

In the fluctuating two-stress repeated block experiments, this damage hypothesis lead to the following simple conditions: (1) the number of damage nuclei initiated in the fracture zone was assumed to be a function of σ_1 only, and (2) damage propagation was assumed to proceed at both σ_1 and σ_2 as shown in figure 6.

The sum of the damage increments ΔD taken alternately at stress levels σ_1 and σ_2 for each increment of cycles ΔN (in fig. 6) until failure is equal to D_f given by equation (3). If $R = r_2/r_1$ and $a_1 = a_2 = a$, the expression for the fatigue life N_g is

$$\frac{N_g}{N_1} = \frac{1}{\alpha + R^{1/a}(1 - \alpha)} \tag{4}$$

If q stress levels (or intervals) are employed, equation (4) becomes

$$\frac{N_g}{N_1} = \frac{1}{\sum_{i=1}^{q} \alpha_i R_i^{1/a}} \tag{5}$$

where N_1 is the life at the highest stress σ_1, and the quantities α_i and $R_i^{1/a}$ correspond to the i^{th} stress level (or interval) σ_i. The detailed mathematical derivation of equations (4) and (5) is given in a previous paper (ref. 3).

The problem of fatigue life under complex stress history was divided into three phases. The first phase for a particular combination of σ_1 and σ_2 was considered and, the assumptions that r was constant for each particular stress and a was constant for all stresses, required a constant value for the quantity $R^{1/a}$, and, therefore, N_g/N_1 was a function of α only. This assumption will be considered in the light of the experimental results. In the second phase of the investigation, σ_1 was maintained constant and σ_2 was varied. A different value of $R^{1/a}$ was expected for each combination of σ_1 and σ_2; however, the number of damage nuclei m_1 was the same because m was a function of σ_1 only. Therefore, $R^{1/a}$ was a function of σ_2/σ_1, and N_g/N_1 was a function of α and $R^{1/a}$. After the relation between $R^{1/a}$ and σ_2/σ_1 was determined using the experimental data, the fatigue life under a continuously varying stress history was calculated. The third phase of the investigation, employing various values of both σ_1 and σ_2, is yet to be considered.

RESULTS AND DISCUSSION

Two-Stress Repeated Block Experiments

The results of the constant stress experiments and the two-stress repeated block experiments for 2024-T4 and 7075-T6 aluminum-alloy wire and hard-drawn-steel wire are tabulated in table I. In this table, the subscript 1 denotes that the quantity is associated with high stress, and the subscript g denotes that the quantity is associated with a complex stress history. The quantities N_1 and N_g are the life of the specimens at high stress and for the complex stress histories, respectively. The mean value of $\log N_g$ was obtained by assuming logarithmic-normal distribution of fatigue life. From the experimental values of N_g and N_1, $R^{1/a}$ was calculated using equation (4) for each experimental condition.

In figure 7 the S-N diagrams are shown for 2024-T4 and 7075-T6 aluminum-alloy wire and hard-drawn-steel wire, respectively. The circular points are the results obtained early in the experimental program, and the triangular points are the results obtained at the end of the

program. The mean endurance limit for the steel wire was determined from 17 specimens by staircase analysis (ref. 2) to be 59,400 psi with a standard deviation of 1900 psi.

Figure 8 shows the diagrams of $(\log N_g - \log N_1)$ against $\log \alpha$ for the three materials. Both mean values and 95-percent confidence limits of $(\log N_g - \log N_1)$ are given for the experimental points. The curves in figure 8 were drawn by using constant values of $R^{1/a}$ for the group of points having the same combination of high and low stress, that is, σ_1 and σ_2. These curves correlate the experimental data very well. The points for α equal to 40 percent exhibit the poorest agreement. The experimental error in α itself may be large in this case and contribute to this error. This will be discussed later. The values of $R^{1/a}$ used in plotting these curves are listed in the $R^{1/a}$ (group) column of table I. The ratio between the experimental life $N_{g,ex}$ and the theoretical life $N_{g,th}$ calculated by using the constant value of $R^{1/a}$ is shown in the $(N_{g,ex}/N_{g,th})$ column of table I. The straight broken line to the right of each of these three figures represents $R^{1/a} = 0$, that is, the damage done by the cycles of low stress is zero. Any point to the right of this line has a negative value of $R^{1/a}$, which implies that a beneficial or strengthening effect was produced by the low-stress cycles.

In figure 8(c), for hard-drawn steel, the experimental points for σ_2 of 28,000 and 20,000 psi are located to the right of the dashed line. The values of $R^{1/a}$ for these points are negative, indicating that a beneficial effect has resulted from these low-stress cycles. This favorable effect is probably due to strain aging of the steel at low stresses. The possible effect of stain aging by these low-stress cycles on further fatigue damage is considered qualitatively in more detail in appendix A.

The values $R^{1/a}$ for the groups of points having the same combination of σ_1 and σ_2 but different values of α were so determined that

$$\sum\left(\frac{N_g}{N_1}\right)_{th} = \sum\left(\frac{N_g}{N_1}\right)_{ex} \tag{6}$$

for each group of points. The value of $(N_g/N_1)_{th}$ was calculated by using equation (4) and the same set of α values as used in the experiments. Since for each material the values of α used were the same through the program, the quantity $\sum\left(\frac{N_g}{N_1}\right)_{th}$ is a function of

$R^{1/a}$ only. Therefore, a theoretical curve of $R^{1/a}$ against $\sum\left(\frac{N_g}{N_1}\right)$ was drawn, and from the known values of $\sum\left(\frac{N_g}{N_1}\right)_{ex}$, the values of $R^{1/a}$ for best fit for each group of points were read off the curve. In this calculation, the values for α equal to 40 percent were not used because they were unreliable. For α equal to 40 percent, only a few revolutions of the large cam were required for fracture. Therefore, the α for the first and the last repeated block for a specimen may be much less than 40 percent. This error is reflected in the longer life of the specimens.

There are other methods that can be used to determine the value of $R^{1/a}$ for each group of points having the same stresses, σ_1 and σ_2. The average of $R^{1/a}$ of the individual points of the group might be used, or the $R^{1/a}$ for the group of points could be determined so that

$$\sum \log\left(\frac{N_g}{N_1}\right)_{th} = \sum \log\left(\frac{N_g}{N_1}\right)_{ex}$$

for this group.

The method used in this investigation emphasized or weighted the points with low values of α_1 because they lead to a narrower permissible range of values of $R^{1/a}$ than the points with high values of α. This method was intended to emphasize the most reliable data in evaluating $R^{1/a}$.

Figure 9(a) shows the plot of $\log R^{1/a}$ against $\log\left(\frac{\sigma_2}{\sigma_1}\right)$ for 2024-T4 aluminum wire. The experimental points lie on a straight line; the slope of the line is 5.778. This suggests that the relation between $R^{1/a}$ and σ_2/σ_1 is in the form of

$$R^{1/a} = \left(\frac{\sigma_2}{\sigma_1}\right)^{5.778} \tag{7}$$

The diagram of $\log R^{1/a}$ against $\log\left(\frac{\sigma_2}{\sigma_1}\right)$ for 7075-T6 aluminum wire is shown in figure 9(b). The experimental points for the higher values of σ_2 fall on a slightly curved line; however, for σ_2 of 25,000 and 20,000 psi, the values of $R^{1/a}$ are very low. Figure 9(c) shows a diagram of $\log R^{1/a}$ against $\log\left(\frac{\sigma_2 - \sigma_0}{\sigma_1 - \sigma_0}\right)$ for 7075-T6 aluminum-alloy wire using a σ_0 value of 15,000 psi. In figure 9(c), the data

exhibit an approximately linear relation. No particular significance was attached to the value of σ_0; however, this relation will be convenient in estimating the life for continuously varying stress histories. The slope of the line is 3.3.

In figure 9(d), only the positive experimental values of $R^{1/a}$ for hard-drawn-steel wire are shown. A straight line can be used to approximate the first four experimental points. The phenomenon of strain-aging apparently influenced the results for σ_2 values of 34,000 psi and lower. Figure 9(e) also shows the values of $R^{1/a}$ against σ_2/σ_1 on a linear scale including negative values for hard-drawn-steel wire.

Continuously Varying Stress Experiment

Based on the relation between $R^{1/a}$ and σ_2/σ_1 obtained experimentally, the life of specimens under continuously varying load can be estimated from equation (5).

One experiment employing continuously varying stress amplitude was completed for 2024-T4 aluminum wire. The stress spectrum limits were from 50,000 to 9,500 psi, and the stress history is shown in figure 4(b). The stress spectrum was divided into 17 intervals, and the mean values of the stress intervals were used to determine the value of $R^{1/a}$ for that stress interval. The relative fraction of life at various stress intervals α_i is shown in figure 10.

The relation between $R^{1/a}$ and σ_2/σ_1 for 2024-T4 aluminum wire is given by equation (7). Substitution of this relation into equation (5), gives

$$N_g = \frac{N_1}{\sum_{i=1}^{q} \alpha_i \left(\frac{\sigma_i}{\sigma_1}\right)^{5.778}} \tag{8}$$

The detailed calculations are tabulated in table II. The estimated life of the specimens with the stress history as shown in figure 4(b) was 3.1×10^5 cycles, and the experimentally determined life was 2.9×10^5 cycles. Thus, excellent agreement was obtained between the results of the two-stress repeated block experiments and the continuously varying stress amplitude experiments. This correlation is very encouraging, however, the results of additional experiments, now in progress, are required to firmly establish this relation.

CONCLUDING REMARKS

The results of the two-stress repeated block experiments for 2024-T4 and 7075-T6 aluminum-alloy and hard-drawn-steel wire established the hypothesis that the fatigue life varies linearly with percent of life at high stress and according to the relation of equation (4).

Equivalently, these results established the fact that for given values of high and low stress one value of the stress interaction parameter adequately represented the interaction between cycles at high and low stress. For the steel wire at low values of low stress, the lives were longer than expected and negative values of the stress interaction parameter were obtained. This phenomenon was attributed to strain-aging or coaxing.

Based on the adequacy of the two-parameter expression given previously, a simple correlation was obtained between the stress interaction parameter $R^{1/a}$ and the high and low stresses σ_1 and σ_2 in order to represent the fatigue life for all of the two-stress repeated block sets of data. The simplest relation between $R^{1/a}$, and σ_1 and σ_2 that adequately represented the data for all three materials was

$$R^{1/a} = \left(\frac{\sigma_2 - \sigma_0}{\sigma_1 - \sigma_0}\right)^d$$

where σ_0 and d are constants. The constants, determined from the experimental data, were

Specimen	d	σ_0, psi
2024-T4 Aluminum-alloy wire	5.778	0
7075-T6 Aluminum-alloy wire	3.30	15,000
Brite basic steel wire	5.98	0

For 2024-T4 aluminum alloy, one experiment was completed employing a continuously varying stress history. The life measured experimentally was in excellent agreement with the life computed using the two expressions previously discussed. Further work of this type is in progress for all three materials. Based on these data, it appears that the results of the two-stress repeated block experiments may be correlated with the results of the continuously varying amplitude experiments.

University of Illinois,
Urbana, Ill., November 4, 1957.

APPENDIX A

ANALYSIS OF STRAIN-AGING IN COLD-DRAWN-STEEL WIRE

During two-stress repeated block experiments, it was observed that for values of low stress σ_2 considerably below the fatigue strength, the fatigue life was longer than would be expected if damage occurred only at the high stress σ_1. This longer life was attributed to strain-aging. Apparently, the strain-aging which occurs at cycles of σ_2 also influences the rate of crack propagation at σ_1. Of the many possible phenomena that may occur, two simple conditions will be examined. It is assumed that strain-aging, that is, pinning of dislocation in the vicinity of the nose of the crack, occurs during cycles of low stress σ_2. During this cycling, crack propagation will be assumed to be zero. As a result of the pinning, crack propagation at σ_1 is also influenced. The stress σ_1 must tear dislocations free from the carbon and nitrogen atmospheres. At least two possibilities exist: (a) all dislocations are pinned and a certain number of cycles of stress are required to free the dislocations, or (b) only a portion of the dislocations are pinned because the magnitude of σ_2 is sufficient to prevent the pinning of some dislocations. However, those dislocations that are pinned are held tightly and even cycles of σ_1 do not free them. Thus, the rate of crack propagation is lower at σ_1 following σ_2 than it would be if the σ_2 cycles were omitted.

These two possibilities are considered as case (a) and (b) in the following:

Case (a)

From equation (3)

$$D_f = m_1 r_1 N_1^{a} \tag{3}$$

where

a constant

m_1 number of damage nuclei at σ_1

N_1 number of cycles to failure at σ_1

r_1 coefficient of crack propagation at σ_1

For two-stress repeated block experiments, it is assumed that

$$r_2 = 0$$

and if the influence of strain-aging during cycles of σ_1 is initially neglected,

$$D_f = m_1 r_1 N_1^a = m_1 r_1 (\alpha N_g)^a \tag{8}$$

where N_g is the fatigue life and α is the percent of cycles at the high stress. With the influence of strain-aging at σ_1 present, the effective cycles during which crack propagation occurs at σ_1 is reduced from αN_g to $(\alpha - \delta)N_g$ where δ is the fraction of cycles in each repeated block required to break free the pinned dislocations. Thus

$$D_f = m_1 r_1 N_1^a = m_1 r_1 (\alpha - \delta) N_g^a \tag{A1}$$

and

$$N_g = \frac{N_1}{\alpha - \delta} \tag{A2}$$

Case (b)

Equations (3) and (8) remain valid in the absence of any influence of strain-aging at σ_1. In the presence of strain-aging, the coefficient of crack propagation r_1 will be reduced from r_1 to βr_1 where

$$\beta < 1$$

because of the reduced number of dislocations that contribute to crack propagation. The expression for damage, with $r_2 = 0$, becomes

$$D_f = m_1 r_1 N_1^a = m_1 r_1 \beta (\alpha N_g)^a \tag{A3}$$

and

$$N_g = \frac{N_1}{\alpha (\beta)^{1/a}} \tag{A4}$$

The results of case (a) and (b) are indicated schematically in figure 11.

It appears that for a σ_2 of 20,000 psi, case (b) is in reasonable agreement with the data in figure 8(c). Case (a) is not in agreement with any of the data. For σ_2 values of 28,000 and 34,000 psi, it appears that r_2 is not zero as assumed, but that the general assumptions made in case (b), with the exception of $r_2 = 0$, may be valid. This does not eliminate other assumptions that lead to the same expression, equation (A4); however, the simple concept that a fraction of the dislocations become pinned and inoperative at σ_2 and σ_1 provides an adequate description based on the very limited data available.

APPENDIX B

COMPARISON OF DATA WITH OTHER THEORIES OF CUMULATIVE FATIGUE DAMAGE

The experimental results of this investigation will be compared with other theories of cumulative fatigue damage that have been proposed. The early theory of references 4 to 6, frequently referred to as the linear summation of "cycle-ratio" hypothesis, may be generalized along lines suggested in references 7 to 10 in order to allow a study of several variations.

Each of these investigations employed the cycle ratio as the basic variable in their theory. Cycle ratio is defined as the ratio n'/N, where N is the average life at stress σ, and n' is the number of cycles $(n' < N)^*$ applied at this stress. Fatigue damage was defined in several ways, however, fracture represented 100-percent damage in all cases.

For a general approach to this problem in terms of the cycle ratio ϕ, assume that the damage D is related to ϕ by the expression

$$D = \phi^{\gamma} \tag{B1}$$

where the exponent γ is a constant for a given stress; however, the value of γ may be different for different stresses.

For two stresses σ_1 and σ_2, $(\sigma_1 > \sigma_2)$, and corresponding fatigue lives, N_1 and $N_2 (N_2 > N_1)$, it was suggested (refs. 7 and 10) that $\gamma_2 > \gamma_1$ appeared to fit some experimental data. The relation (eq. (B1)) between damage D and cycle ratio ϕ is shown schematically in figure 12 for the two-stress repeated block load history employed in most of the data included in this report. Initially αn^* cycles of high stress σ_1 were applied, followed by $(1 - \alpha)n$ cycles of low stress σ_2, and so forth. The path of damage accumulation is indicated by the heavy solid line in figure 12.

The various increments of damage ΔD are given by the product of the slope of the damage curve in the interval considered $dD/d\phi$ and the cycle-ratio increment $\Delta\phi$, that is,

$$\Delta D_i^j = \left.\frac{dD}{d\phi}\right|_i \Delta\phi = \gamma \phi^{\gamma - 1} \Delta\phi \tag{B2}$$

---

*n' is employed in the definition of the cycle ratio to avoid confusion with the quantity n which is the length of each repeated block used in this report.

In terms of the two-stress repeated block loading employed in the present experiment, the various values of ΔD are

$$\Delta D_0{}^a = r_1\left(\frac{0}{N_1}\right)^{r_1-1}\frac{\alpha n}{N_1}$$

$$\Delta D_b{}^c = r_2\left(\frac{\alpha n}{N_2}\right)^{r_2-1}\frac{(1-\alpha)n}{N_2}$$

$$\Delta D_d{}^e = r_1\left(\frac{n}{N_1}\right)^{r_1-1}\frac{\alpha n}{N_1}$$

$$\Delta D_f{}^h = r_2\left(\frac{n+\alpha n}{N_2}\right)^{r_2-1}\frac{(1-\alpha)n}{N_2}$$

$$\Delta D_i{}^j = r_1\left(\frac{2n}{N_1}\right)^{r_1-1}\frac{\alpha n}{N_1}$$

$$\Delta D_k{}^l = r_2\left(\frac{2n+\alpha n}{N_2}\right)^{r_2-1}\frac{(1-\alpha)n}{N_2}$$

and so forth.

The total damage D is given by the sum of the damage increments ΔD as follows:

$$D = \sum_1^g \Delta D = r_1\left(\frac{0\times n}{N_1}\right)^{r_1-1}\frac{\alpha n}{N_1} + r_2\left(\frac{\alpha n}{N_2}\right)^{r_2-1}\frac{(1-\alpha)n}{N_2} + r_1\left(\frac{n}{N_1}\right)^{r_1-1}$$

$$\frac{\alpha n}{N_1} + r_2\left(\frac{n+\alpha n}{N_2}\right)^{r_2-1}\frac{(1-\alpha)n}{N_2} + r_1\left(\frac{2n}{N_1}\right)^{r_1-1}\frac{\alpha n}{N_1} + r_2\,\frac{2n+\alpha n}{N_2}^{\,r_2-1}$$

$$\frac{(1-\alpha)n}{N_2} + \cdots + r_1\left(\frac{gn}{N_1}\right)^{r_1-1}\frac{\alpha n}{N_1} + r_2\left(\frac{gn+\alpha n}{N_2}\right)^{r_2-1}\frac{(1-\alpha)n}{N_2} \quad \text{(B3)}$$

At failure, $D = 1$, and this expression can be rearranged and simplified to the form

$$D = 1 = \frac{r_1 \alpha n^{r_1}}{(N_1)^{r_1}} \left[0 + 1^{r_1-1} + 2^{r_1-1} + 3^{r_1-1} + \ldots + (g)^{r_1-1}\right] +$$

$$\frac{r_2(1-\alpha)n^{r_2}}{(N_2)^{r_2}} \left[\alpha^{r_2-1} + (1+\alpha)^{r_2-1} + (2+\alpha)^{r_2-1} + (3+\alpha)^{r_2-1} + \ldots . \right.$$

$$\left. + (g+\alpha)^{r_2-1}\right] \qquad \text{(B4)}$$

For failure after a few repeated blocks of cycles (say $g < 10$) it is possible to compute the sum of the series of terms in equation (B4). For large values of g, which are of primary interest here, the series of terms may be evaluated by integration, thus equation (B4) becomes

$$D = 1 = \frac{r_1 \alpha n^{r_1}}{(N_1)^{r_1}} \int_0^g x^{r_1-1}\, dx + \frac{r_2(1-\alpha)n^{r_2}}{(N_2)^{r_2}} \int_0^g (x+\alpha)^{r_2-1}\, dx$$

which gives

$$D = 1 = \frac{r_1 \alpha n^{r_1}}{(N_1)^{r_1}} \left(\frac{g^{r_1}}{r_1}\right) + \frac{r_2(1-\alpha)n^{r_2}}{(N_2)^{r_2}} \left[\frac{(g+\alpha)^{r_2} - \alpha^{r_2}}{r_2}\right] \qquad \text{(B5)}$$

Since $\alpha < 1$ and g is large, the quantities α^{r_2} and α in the last bracket will be neglected, so that

$$1 = \alpha\left(\frac{ng}{N_1}\right)^{r_1} + (1-\alpha)\left(\frac{ng}{N_2}\right)^{r_2}$$

The quantity ng is the fatigue life N_g for the two-stress repeated block loading, thus

$$1 = \alpha\left(\frac{N_g}{N_1}\right)^{r_1} + (1-\alpha)\left(\frac{N_g}{N_2}\right)^{r_2} \qquad \text{(B6)}$$

The various possible cases contained in equation (B6) will now be considered.

Case A; $r_1 = r_2 = 1$

Equation (B6) reduces to the linear summation of cycle-ratio hypothesis, and may be written as

$$\frac{N_g}{N_1} = \frac{1}{\alpha + (1 - \alpha)\left(\frac{N_1}{N_2}\right)} \tag{B7}$$

In figure 13, the solid lines represent the values of the ratio N_g/N_1 given by equation (B7) for aluminum alloy 2024-T4 for two-stress repeated block loading. The results are shown for a high stress of 50,000 psi and low stresses of 45,000, 40,000, 35,000, and 30,000 psi. Values of the quantity $\sum n/N$ are given in table I for the three materials reported for all combinations in which N_2, the life at the low stress, was determined. While a few of the experimental data are adequately represented by the solid lines in figure 13, it is evident that for values of σ_2 close to σ_1, the solid line gives unconservative values of life, but conversely for low values of σ_2, the solid line estimates a life that is too short. If values of N_2 for σ_2 of 25,000 and 20,000 psi are obtained by extrapolation of the S-N diagram in figure 7(a) and substituted into equation (B7), the difference between the solid line and the data becomes increasingly greater as σ_2 becomes smaller. Because of the uncertainty of the extrapolated values of N_2, they were not included in figure 13 or table I. It appears evident from figure 13, however, that while equation (B7) may give reasonable values in isolated cases, errors on either the long-life or short-life side occur in numerous other instances. (See table I.) Thus the analysis of cumulative damage given by equation (4) or (5) of this report provides a more reliable approach to this problem without introducing undue complications.

Case B; $r_1 = r_2 > 1$

Equation (B6) becomes

$$\frac{N_g}{N_1} = \left[\frac{1}{\alpha + (1 - \alpha)\left(\frac{N_1}{N_2}\right)^r}\right]^{1/r} \tag{B8}$$

Equation (B8) is a generalized form of the relation proposed in references 8 and 9. From references 8 and 9, an expression for the "reduced stress" S_r is

$$S_r = \left(\frac{\sum \Delta n_i S_i^{2x}}{\sum \Delta n_i} \right)^{1/2x}$$

where the life at S_r is the same as for the spectrum loading. The expression for the S-N curves is (refs. 8 and 9)

$$S = \frac{B'}{N^{1/x}}$$

where B' is a constant, and x is the slope of the S-N curve plotted on a double logarithmic diagram. An introduction of the symbols employed in this report leads to the following relations:

$$S_r = \frac{B'}{N_g^{1/x}}$$

and

$$\sum \Delta n_1 S_i^{2x} = \alpha N_g \left(\frac{B'}{N_1^{1/x}} \right)^{2x} + (1 - \alpha) N_g \left(\frac{B'}{N_2^{1/x}} \right)^{2x}$$

and

$$\sum \Delta n_i = N_g$$

Substitution of these expressions simplifies the equation of references 8 and 9 for the reduced stress:

$$\frac{N_g}{N_1} = \left[\frac{1}{\alpha + (1 - \alpha) \left(\frac{N_1}{N_2} \right)^2} \right]^{1/2} \tag{B9}$$

This expression is identical to equation (B8) for the value, $\gamma = 2$.

Comparison of the lives given by equation (B9) with the experimental data for 2024-T4 aluminum alloy is shown in figure 14 for σ_1 of 50,000 psi and σ_2 of 45,000, 40,000, 35,000, and 30,000 psi. For σ_2 of 45,000 psi the agreement is good, however, the agreement decreases for the lower values of σ_2. As the limiting case, when N_2

becomes very large, the straight line in figure 14 indicates lives that are much too short. This line has a slope $1/\gamma$, which indicates that for values of $\gamma > 2$, the agreement would be even less. The lives for all values of σ_2 are bounded on the short-life side by the vertical line, $\log N_g - \log N_1 = 0$, and on the long-life side by a line through the origin with a slope $-1/\gamma$. This indicates that the best agreement with the experimental data is obtained from equation (B8) when $\gamma = 1$, which then reduces to equation (B7), the linear summation of cycle ratios. However, this conclusion is restricted to the case $\gamma_1 = \gamma_2$. It is necessary now to examine the results for $\gamma_1 \neq \gamma_2$.

Case C; $\gamma_1 \neq \gamma_2$

Case C gives the form of the equations proposed by references 7 and 10.

It is convenient to first consider the limiting condition, that is, when N_2 is very large. Rewriting equation (B6) gives

$$1 = \alpha\left(\frac{N_g}{N_1}\right)^{\gamma_1} + (1 - \alpha)\left(\frac{N_g}{N_2}\right)^{\gamma_2} \qquad \text{(B6)}$$

The second term on the right side approaches zero when N_2 becomes very large. Therefore, the influence of the value of γ_1 may be examined independently in this limiting condition. Solving for N_g/N_1 gives

$$\frac{N_g}{N_1} = \frac{1}{\alpha^{1/\gamma}} = \alpha^{-1/\gamma}$$

This relation defines a straight line through the origin in figure 15, with a slope of $-1/\gamma$, similar to the situation discussed under case B. It is evident from an examination of figures 8 and 15 that the only value of γ_1 that gives reasonable fit to the data is $\gamma_1 = 1.0 \pm 0.1$. With the required value of γ_1 established to fit all of these data, it is now necessary to examine the influence of γ_2.

Equation (B6) was solved employing the following values: $\gamma_1 = 1$ and $\gamma_2 = 1$, 2, and 4. These results are plotted in figure 15 for aluminum alloy 2024-T4 for the two-stress repeated block loading. As before, the data are included for a high stress of 50,000 psi and low stresses of 45,000, 40,000, 35,000, and 30,000 psi. There are several instances in which the lines for $\gamma_2 = 2$ or $\gamma_2 = 4$ appear to fit some of the data well. However, in no instance does any one of these

curves fit the data for the range of α values and for a given combination of high and low stress as well as the solid curves in figure 8(a).

There are two important points to be noted. First, the lines in figures 13, 14, and 15, obtained from equations (B7), (B9), and (B6), respectively, each employ the cycle ratio ϕ at both the high and low stress as a fundamental variable. Based on this assumption that the cycle ratio is a fundamental variable, the theoretical expressions must give values that lie on some smooth curve connecting the end points, $(\log N_g - \log N_1) = 0$ for $\alpha = 1.00$ and $(\log N_g - \log N_1) = (\log N_2 - \log N_1)$ for $\alpha = 0$. This requirement is well illustrated in figure 15. When these end-point restrictions are imposed, the possible variation in the shape of the curves is limited and it is not possible to fit the experimental data adequately. Simply by eliminating the cycle ratio ϕ at the low stress as a fundamental variable, the possibility of fitting the data is greatly increased, as shown by the good fit (fig. 8) obtained in this report.

The second important point is that the new analytical expression, equation (4) or (5), contains an additional parameter $R^{1/a}$. The excellent correlation between the data and equations (4) and (5) establishes the fact that the introduction of this one additional parameter provides adequate flexibility to fit all of the data collected in this investigation. The evaluation of the $R^{1/a}$ parameter and correlation with the ratio of stresses σ_2/σ_1 by an expression of the type

$$R^{1/a} = \left(\frac{\sigma_2}{\sigma_1}\right)^d$$

was adequately considered for the wire data in this report. Evaluation of the parameter $R^{1/a}$ for other specimen configurations and stress ranges will be considered in a later report.

It is interesting and encouraging to note that in reference 11 essentially the same analytical expression for fatigue life due to a spectrum of random load amplitudes was developed.

REFERENCES

1. Southwell, R. V.: An Introduction to the Theory of Elasticity for Engineers and Physicsts. Clarendon Press (Oxford), 1936.

2. Corten, H. T., and Sinclair, G. M.: A Wire Fatigue Machine for Investigation of the Influence of Complex Stress Histories. Proc. ASTM, vol. 56, 1956, pp. 1124-1137.

3. Corten, H. T., and Dolan, T. J.: Cumulative Fatigue Damage. The International Conf. on Fatigue of Metals, Inst. Mech. Eng. (London), and ASME (N.Y.), Sept. 10-14, 1956.

4. Palmgren, Arvid: Die Lebensdauer von Kugellagern. Z.V.D.I., Bd. 68, No. 14, Apr. 5, 1924, pp. 339-341.

5. Langer, B. F.: Fatigue Failure from Stress Cycles of Varying Amplitude. Jour. Appl. Mech., vol. 4, no. 4, Dec. 1937, pp. A160-A162.

6. Miner, Milton A.: Cumulative Damage Fatigue. Jour. Appl. Mech., vol. 12, no. 3, Sept. 1945, pp. A159-A164.

7. Richart, F. E., Jr., and Newmark, N. M.: An Hypothesis for the Determination of Cumulative Damage in Fatigue. Proc. ASTM, vol. 48, 1948, pp. 1-31; discussion, pp. 32-33.

8. Shanley, F. R.: A Proposed Mechanism of Fatigue Failure. Colloguium on Fatigue, Waloddi Weibull and Folke K. G. Odqvist, eds., Springer-Verlag, 1956, pp. 251-259.

9. Shanley, F. R.: A Theory of Fatigue Based on Unbonding During Reversed Slip. Rep. P-350, The Rand Corp., Nov. 11, 1952. (See also P-350 Supp., May 1, 1953.)

10. Marco, S. M., and Starkey, W. L.: A Concept of Fatigue Damage. Trans. ASME, vol. 76, no. 4, May 1954, pp. 627-632.

11. Freudenthal, A. M.: The Safety of Aircraft Structures. Tech. Rep. 57-131, WADC, July 1957.

TABLE I. - SUMMARY AND ANALYSIS OF FATIGUE LIFE DATA

(a) 2024-T4 Aluminum alloy (machine 3)

High stress, σ_1, psi	Low stress, σ_2, psi	Percent of life at high stress, α	$\log N_g$		Standard deviation	$\log N_g - \log N_1$		$R^{1/a}$, individual points	$R^{1/a}$, group	$\frac{N_{g,e}}{N_{g,t}}$ (a)	$\Sigma \frac{n_i}{N_i}$ (b)	Number of specimens
			Mean	±95-Percent confidence limit		Mean	±95-Percent confidence limit					
50×10^3		100	4.2085	0.0194	0.0415							20
45			4.5771	.0264	.0565							20
40			4.7972	.0340	.0727							20
35			5.0937	.0196	.0380							17
30			5.3897	.0338	.0721							20
50	45×10^3	40	4.4824	.0395	.0845	0.2739	0.0310	0.2202	0.475	1.29	1.23	20
		10	4.5161	.0254	.0542	.3076	.0225	.4361		1.07	.99	20
		3.9	4.5664	.0197	.0408	.3579	.0195	.4158		1.13	1.03	19
		.75	4.4902	.0290	.0620	.2827	.0245	.5192		.92	.83	20
		.32	4.4753	.0235	.0502	.2668	.0214	.5396		.88	.79	20
50	40	40	4.5757	.0267	.0571	.3672	.0232	.0488	.260	1.30	1.29	20
		10	4.7352	.0401	.0621	.5267	.0246	.2193		1.12	1.12	20
		3.9	4.7641	.0297	.0634	.5568	.0249	.2490		1.04	1.03	20
		.75	4.7541	.0192	.0411	.5476	.0192	.2793		.93	.92	20
		.32	4.7540	.0398	.0851	.5456	.0218	.2824		.92	.91	20
50	35	40	4.6077	.0259	.0553	.3993	.0227	-.002	.117	1.18	1.20	20
		10	4.9445	.0263	.0560	.7381	.0229	.0929		1.12	1.18	20
		3.9	5.0273	.0336	.0717	.8188	.0273	.1174		1.00	1.08	20
		.75	5.0859	.0320	.0684	.8775	.0263	.1260		.93	1.03	20
		.32	5.1331	.0420	.0873	.9246	.0322	.1162		1.01	1.12	19
50	30	40	4.6919	.0208	.0445	.4834	.0200	-.119	.050	1.31	1.34	20
		10	5.0595	.0356	.0551	.8511	.0227	.0454		1.03	1.13	20
		3.9	5.3047	.0177	.0377	1.0963	.0185	.0428		1.09	1.27	20
		.75	5.4242	.0240	.0513	1.2167	.0217	.0538		.94	1.20	20
		.32	5.4846	.0349	.0746	1.2761	.0281	.0499		1.00	1.30	20
50	25	40	4.6762	.0234	.0499	.4677	.0214	-.099	.0181	1.21		20
		10	5.1428	.0202	.0432	.9344	.0197	.0181		1.00		20
		3.9	5.4472	.0227	.0485	1.2387	.0210	.0195		.98		20
		.75	5.7765	.0251	.0490	1.5679	.0221	.0197		.94		17
		.32	5.9088	.0287	.0557	1.7003	.0239	.0168		1.07		17
50	20	40	4.6391	.0263	.0562	.4307	.0230	-.049	.00647	1.09		20
		10	5.1559	.0268	.0573	.9474	.0233	.0143		.94		20
		3.9	5.5311	.0185	.0396	1.3226	.0189	.0089		.96		20
		.75	6.0197	.0283	.0532	1.8112	.0236	.0080		.90		16
		.32	6.2560	.0362	.0599	2.0476	.0267	.0057		1.08		13

[a] $N_{g,e}$ and $N_{g,t}$ are the experimental and computed values, respectively.

[b] Values of the linear summation of cycle ratio.

TABLE I. - Continued. SUMMARY AND ANALYSIS OF FATIGUE LIFE DATA

(b) 7075-T6 Aluminum alloy (machine 4)

High stress, σ_1, psi	Low stress, σ_2, psi	Percent of life at high stress, α	$\log N_g$		Standard deviation	$\log N_g - \log N_1$		$R^{1/a}$, individual points	$R^{1/a}$, group	$\frac{N_{g,e}}{N_{g,t}}$ (a)	$\Sigma \frac{n_i'}{N_1}$ (b)	Number of specimens
			Mean	±95-Percent confidence limit		Mean	±95-Percent confidence limit					
50×10^3		100	4.2224	0.0148	0.0317							20
45			4.4113	.0301	.0644							20
40			4.6454	.0308	.0658							20
35			4.9121	.0253	.0541							20
30			5.1731	.0200	.0427							20
50	45×10^3	40	4.3837	.0222	.0474	0.1612	0.0181	0.4832	0.588	1.09	1.14	20
		10	4.4099	.0330	.0707	.1875	.0250	.6104		.97	1.05	20
		3.9	4.4550	.0224	.0480	.2323	.0182	.5687		1.03	1.13	20
		.91	4.4188	.0240	.0513	.1964	.0192	.6348		.93	1.02	20
		.34	4.4851	.0318	.0684	.2626	.0243	.5448		1.08	1.19	20
50	40	40	4.4503	.0231	.0495	.2279	.0186	.3197	.348	1.03	1.06	20
		10	4.6249	.0345	.0737	.4025	.0259	.3287		1.04	1.11	20
		3.9	4.6139	.0327	.0415	.3915	.0165	.3818		.92	.99	20
		.91	4.6538	.0225	.0481	.4314	.0187	.3646		.96	1.03	20
		.34	4.6998	.0286	.0615	.4774	.0222	.3309		1.05	1.14	20
50	35	40	4.5915	.0258	.0551	.3690	.0203	.0458	.1650	1.17	1.22	20
		10	4.8280	.0313	.0674	.6056	.0239	.1643		1.00	1.14	20
		3.9	4.9531	.0508	.0790	.7307	.0275	.1529		1.06	1.27	20
		.91	4.9501	.0734	.0785	.7276	.0274	.1798		.92	1.15	20
		.34	5.0379	.0279	.0595	.8154	.0216	.1501		1.10	1.35	20
50	30	40	4.6118	.0223	.0478	.3893	.0180	.0135	.0627	1.07	1.14	20
		10	5.0326	.0371	.0795	.8101	.0277	.0609		1.01	1.30	20
		3.9	5.2654	.0241	.0515	1.0430	.0193	.0537		1.10	1.62	20
		.91	5.3532	.0260	.0495	1.1307	.0192	.0655		.96	1.62	18
		.34	5.3925	.0274	.0585	1.1700	.0211	.0644		.97	1.70	20
50	25	40	4.7478	.0168	.0360	.5254	.0150	-.170	.0104	1.34		20
		10	5.1735	.0121	.0259	.9511	.0125	.0132		.98		20
		3.9	5.4807	.0210	.0450	1.2583	.0174	.0169		.89		20
		.91	5.9337	.0319	.0680	1.7112	.0242	.0104		1.00		20
		.34	6.1080	.0268	.0557	1.8855	.0209	.0096		1.06		19
50	20	40	4.7529	.0190	.0407	.5305	.0162	-.175	.00243	1.36		20
		10	5.1522	.0309	.0660	.9298	.0236	.0195		.85		20
		3.9	5.5815	.0298	.0639	1.3591	.0229	.0049		.95		20
		.91	6.1384	.0252	.0490	1.9159	.0186	.0030		.95		17
		.34	6.4743	.0494	.0870	2.2519	.0332	.0022		1.04		15

[a] $N_{g,e}$ and $N_{g,t}$ are the experimental and computed values, respectively.

[b] Values of the linear summation of cycle ratio.

TABLE I. - Concluded. SUMMARY AND ANALYSIS OF FATIGUE LIFE DATA

(c) Hard-drawn-steel wire

High stress, σ_1, psi	Low stress, σ_2, psi	Percent of life at high stress, α	$\log N_g$		Standard deviation	$\log N_g - \log N_1$		$R^{1/a}$, individual points	$R^{1/a}$, group	$\frac{N_{g,e}}{N_{g,t}}$ (c)	$\Sigma \frac{n_i}{N_i}$ (d)	Number of specimens	Test series (e)
			Mean	±95-Percent confidence limit		Mean	±95-Percent confidence limit						
96×10^3		100	4.3906	0.0178	0.0440							26	A
86		100	4.6670	.0570	.0680							26	A
76		100	5.0821	.0295	.0730							26	A
66		100	5.5481	.0358	.0885							26	A
96		100	4.4226	.0316	.0570							15	B
96	76×10^3	40	4.7451	.0255	.0546	0.3544	0.0219	0.0702	0.2140	1.20	1.18	20	A
		10	4.9246	.0237	.0507	.5340	.0210	.2138		1.00	.97	20	A
		3.75	4.9871	.0272	.0584	.5965	.0228	.2241		.96	.92	20	A
		.9	5.0601	.0354	.0664	.6695	.0260	.2069		1.03	.98	16	A
96	66	40	4.7637	.0236	.0507	.3730	.0210	.0393	.0980	1.08	1.04	20	A
		10	5.1027	.0218	.0426	.7121	.0200	.1046		.97	.84	17	A
		3.75	5.2859	.0291	.0566	.8633	.0298	.1051		.97	.80	17	B
		.9	5.4122	.0478	.0323	.9896	.0231	.0943		1.04	.81	20	B
96	56	40	4.7865	.0252	.0540	.3959	.0218	.0032	.0433	1.06		20	A
		10	5.2788	.0165	.0382	.8882	.0178	.0327		1.07		23	A
		3.8	5.4412	.0313	.0609	1.0506	.0243	.0530		.90		17	A
		.9	5.7246	.0300	.0640	1.3020	.0303	.0413		1.04		20	B
96	46	40	4.8136	.0323	.0692	.4230	.0255	-.0373	.0148	1.08		20	A
		10	5.3843	.0418	.0844	.9937	.0300	.0016		1.12		18	A
		3.8	5.6497	.0234	.0455	1.2536	.0206	.0178		.95		17	A
		.9	6.0467	.0370	.0720	1.6241	.0342	.0149		1.00		17	B
96	34	40	4.8398	.0340	.0709	.4492	.0262	-.0742	.00127	1.12		19	A
		10	5.4816	.0445	.0928	1.0909	.0320	-.0210		1.23		19	A
		3.8	5.8413	.0192	.0576	1.4507	.0235	-.0027		1.07		17	A
		.9	6.3879	.0488	.0393	1.9653	.0341	.0019		.83		5	B
96	28	40	4.8911	.0388	.0829	.4685	.0356	-.1000	-.00182	1.17		20	B
		10	5.5518	.0495	.0967	1.1612	.0339	-.0344		1.45		17	A
		3.8	5.8897	.0299	.0581	1.4990	.0236	-.0065		1.20		17	A
		.9	6.5391	.0811	.0653	2.1165	.0428	-.0014		1.18		5	B
96	20	40	4.8626	.0472	.0922	.4720	.0327	-.1035	-.00388	1.18		17	A
		10	5.6042	.0334	.0653	1.2136	.0254	-.0432		1.64		17	A
		3.8	5.9837	.0236	.0503	1.5930	.0217	-.0130		1.49		17	A
		.9	6.6748	.0266	.0676	2.2522	.0437	-.0034		1.61		5	B

[c] $N_{g,e}$ and $N_{g,t}$ are the experimental and computed values, respectively. For σ_2 = 20,000, 28,000, and 34,000 psi, the value of $N_{g,t}$ was computed using $R^{1/a} = 0$. (See appendix A)

[d] Values of the linear summation of cycle ratio hypothesis.

[e] The values of log N_g and log N_1 from the same series were used to compute (log N_g - log N_1).

TABLE II. - CALCULATION OF THE FATIGUE LIFE FOR THE CONTINUOUSLY VARYING STRESS HISTORY EXPERIMENT

[2024-T4 Aluminum alloy wire; machine 3; σ_1, 50,000 psi; d, 5.778; $N_1 = 1.62 \times 10^4$ cycles.]

Stress-ratio increment	$\left(\frac{\sigma_i}{\sigma_1}\right)_{mean}$	$\left(\frac{\sigma_i}{\sigma_1}\right)^d$	Number of cycles	α_i	$\alpha_i \left(\frac{\sigma_i}{\sigma_1}\right)^d$
0.95 - 1.00	0.975	0.863	224	0.0224	0.01933
.90 - .95	.925	.637	101	.0101	.00643
.85 - .90	.875	.462	94	.0094	.00434
.80 - .85	.825	.332	84	.0084	.00279
.75 - .80	.775	.232	81	.0081	.00188
.70 - .75	.725	.157	367	.0367	.00576
.65 - .70	.675	.104	373	.0373	.00388
.60 - .65	.625	.066	369	.0369	.00243
.55 - .60	.575	.0411	366	.0366	.00150
.50 - .55	.525	.0241	360	.0360	.00087
.45 - .50	.475	.0136	925	.0925	.00126
.40 - .45	.425	.00707	1205	.1205	.00085
.35 - .40	.375	.00346	1158	.1158	.00040
.30 - .35	.325	.00151	1156	.1156	.00017
.25 - .30	.275	.00059	1225	.1225	.00007
.20 - .25	.225	.00018	1476	.1476	.00003
.19 - .20	.195	.000063	416	.0416	.00000
					0.05199

$$\Sigma \alpha_i \left(\frac{\sigma_i}{\sigma_1}\right)^d = 0.05199$$

$$N_g = \frac{N_1}{\Sigma \alpha_i \left(\frac{\sigma_i}{\sigma_1}\right)^d} = \frac{1.62 \times 10^4}{0.05199} = 3.11 \times 10^5 \text{ cycles}$$

The experimentally determined life was

$$N_g = 2.94 \times 10^5 \text{ cycles}$$

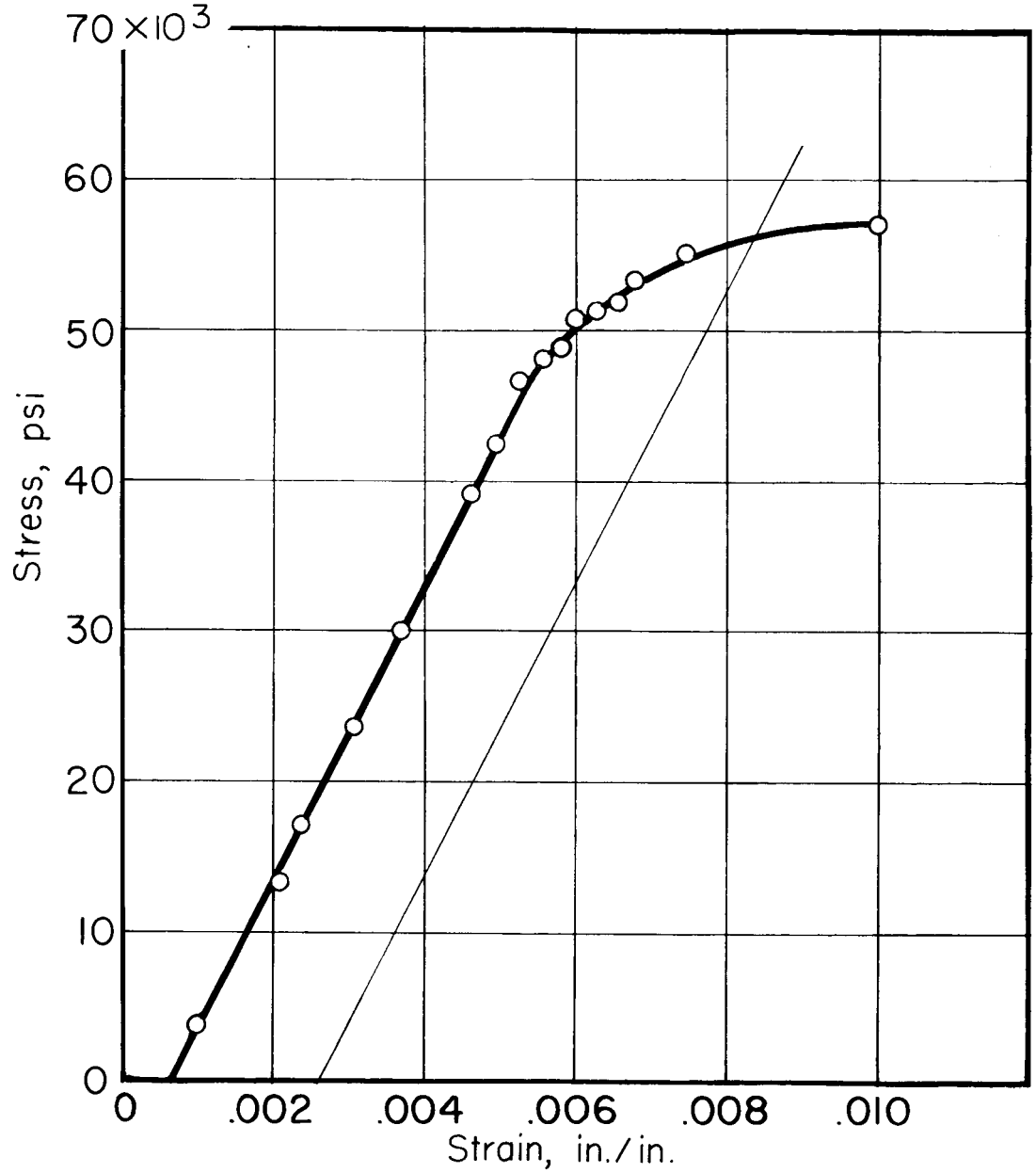

(a) Diagram for 2024-T4 aluminum-alloy wire.

Figure 1.- Stress-strain diagram.

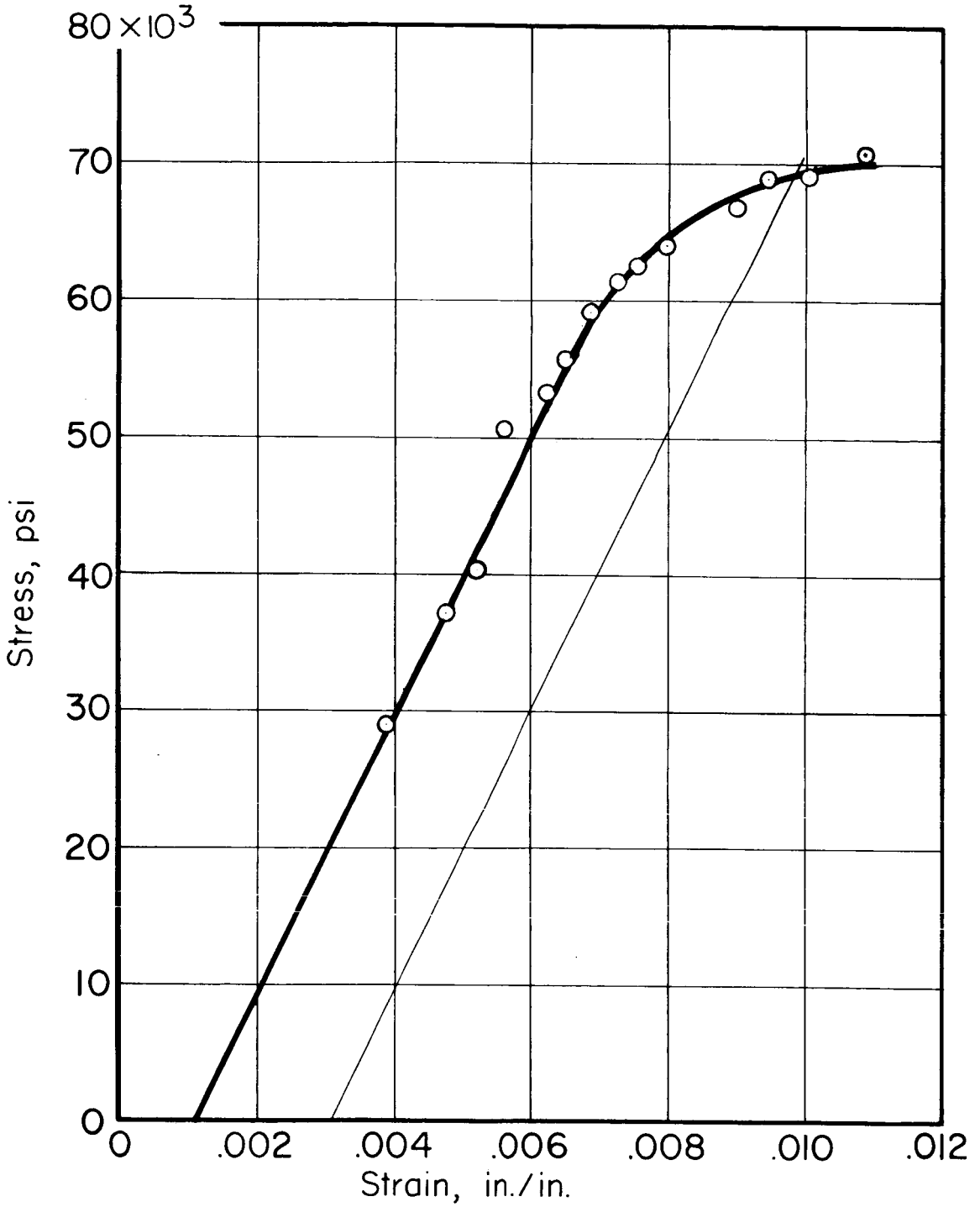

(b) Diagram for 7075-T6 aluminum-alloy wire.

Figure 1. - Continued.

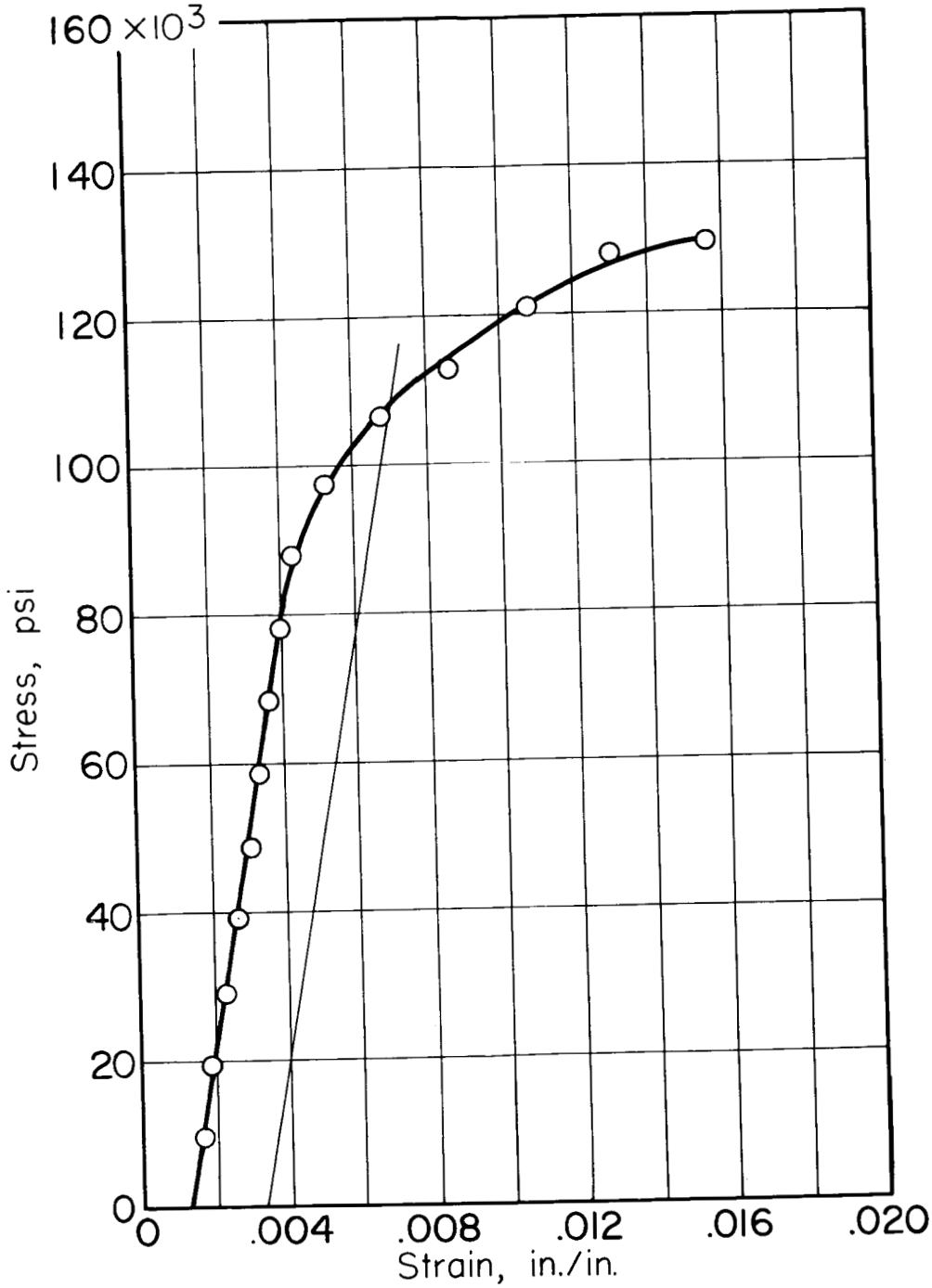

(c) Diagram for hard-drawn steel wire.

Figure 1.- Concluded.

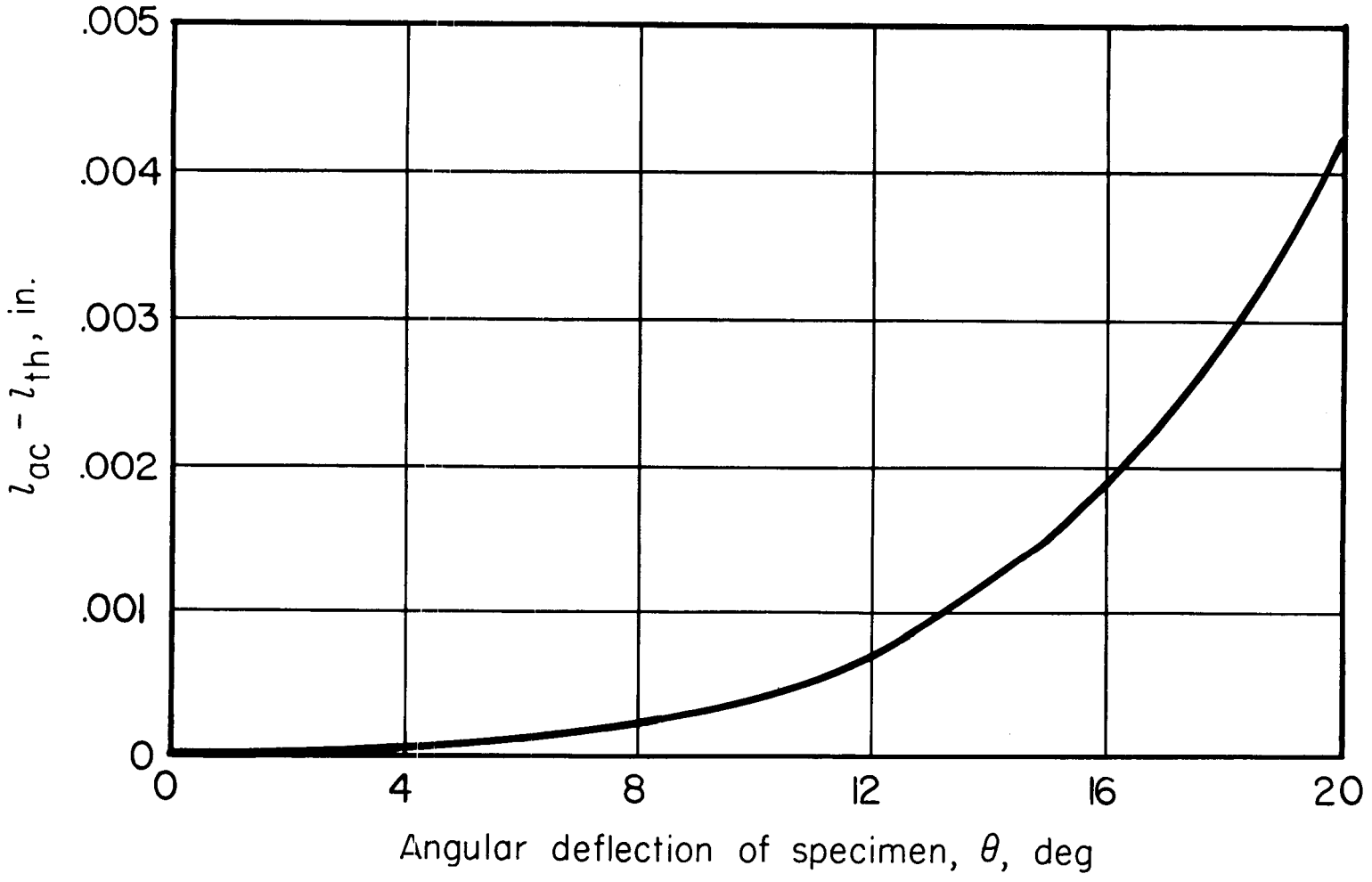

(a) Difference in length of deflected specimen between the theoretical and circular-arc tracks.

Figure 2. - Study of theoretical and circular-arc tracks.

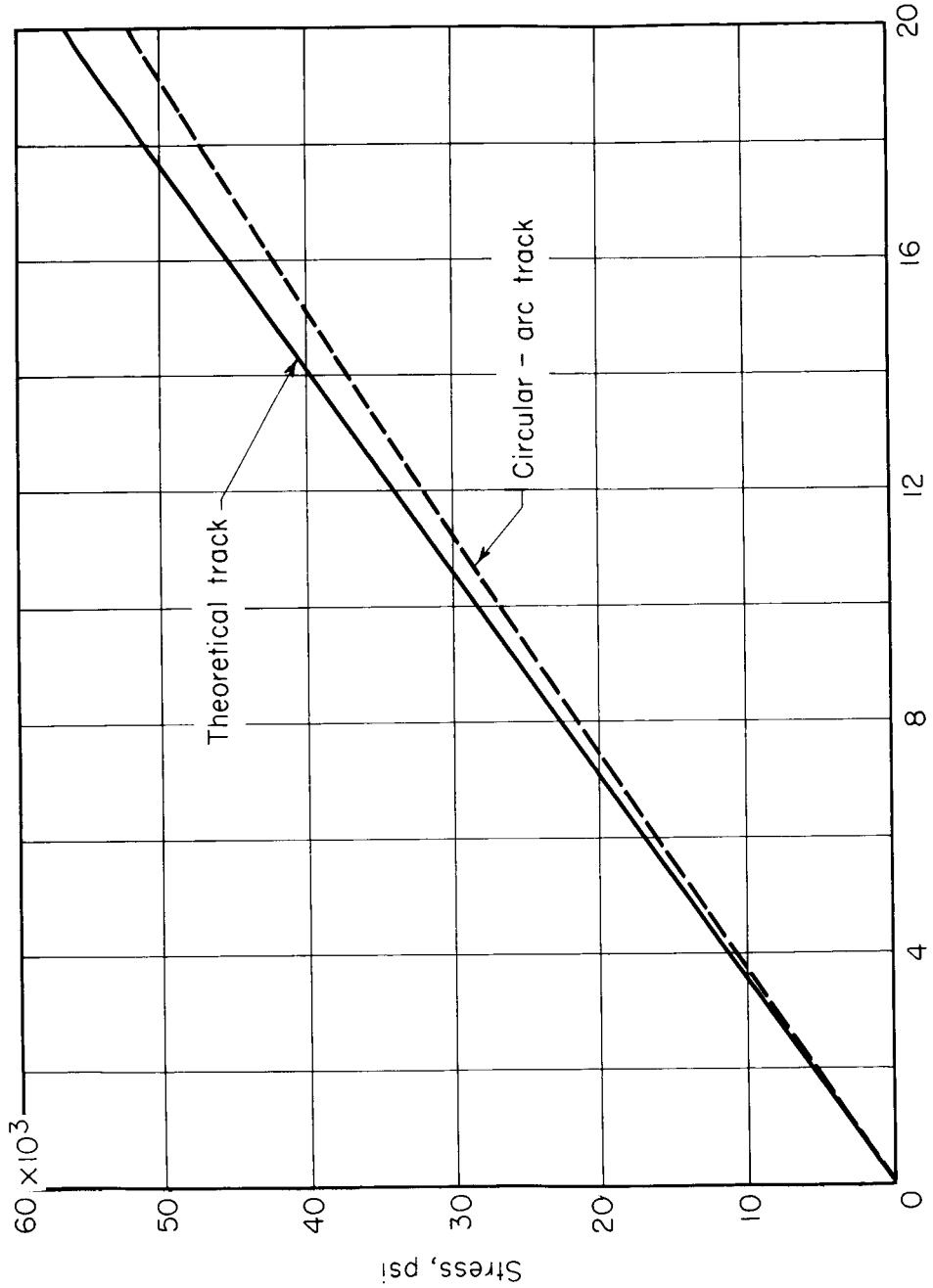

(b) Comparison of computed values for stress.

Figure 2.- Concluded.

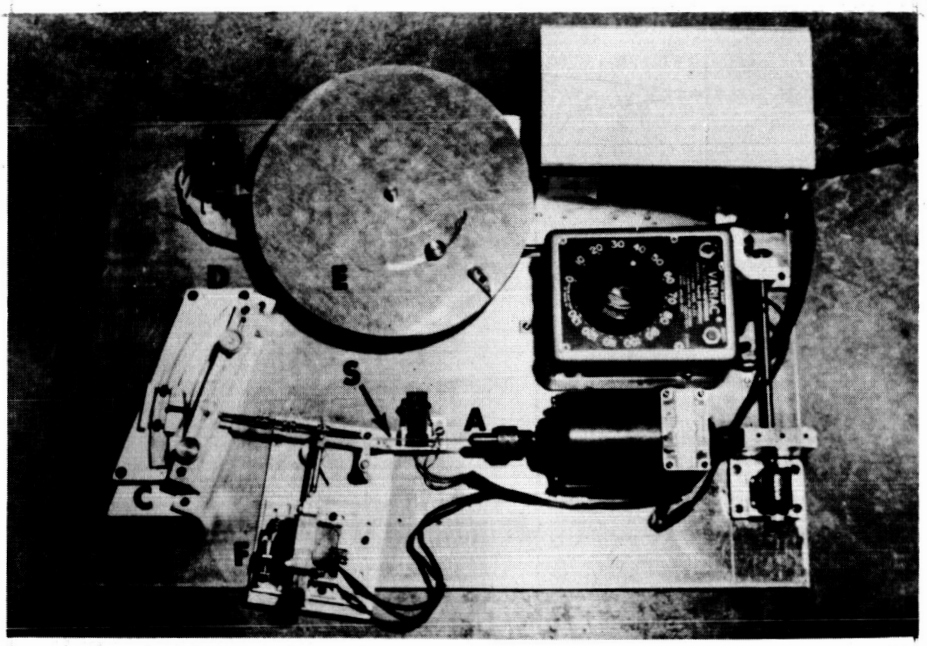

(a) Setup for two-stress repeated block experiments.

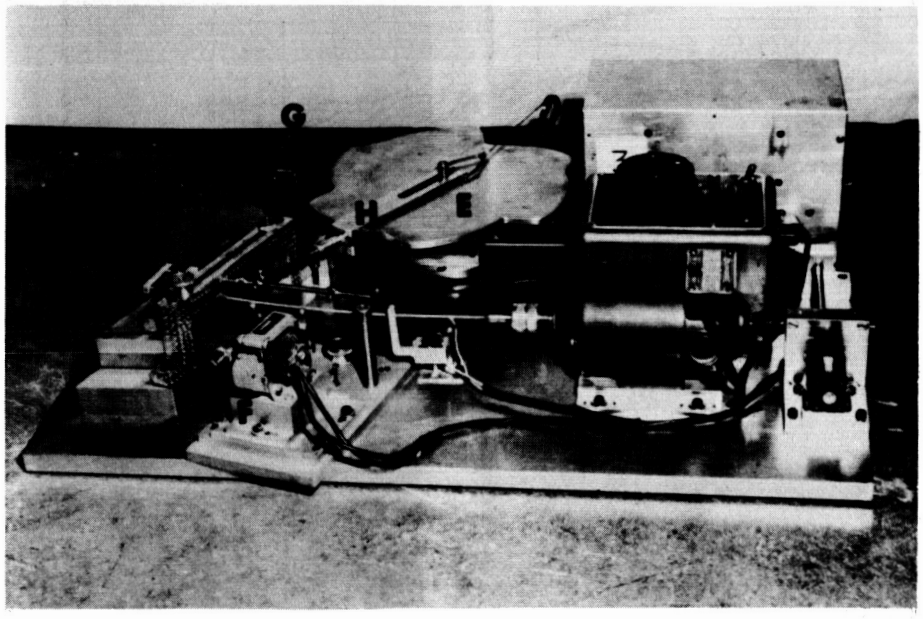

(b) Setup for continuously varying stress experiments.

Figure 3.- Wire fatigue machine equipped for fluctuating load experiments. S, specimen; A, chuck; B, trolley; CD, circular track; E, cam; F, solenoid; G, microswitch; H, follower.

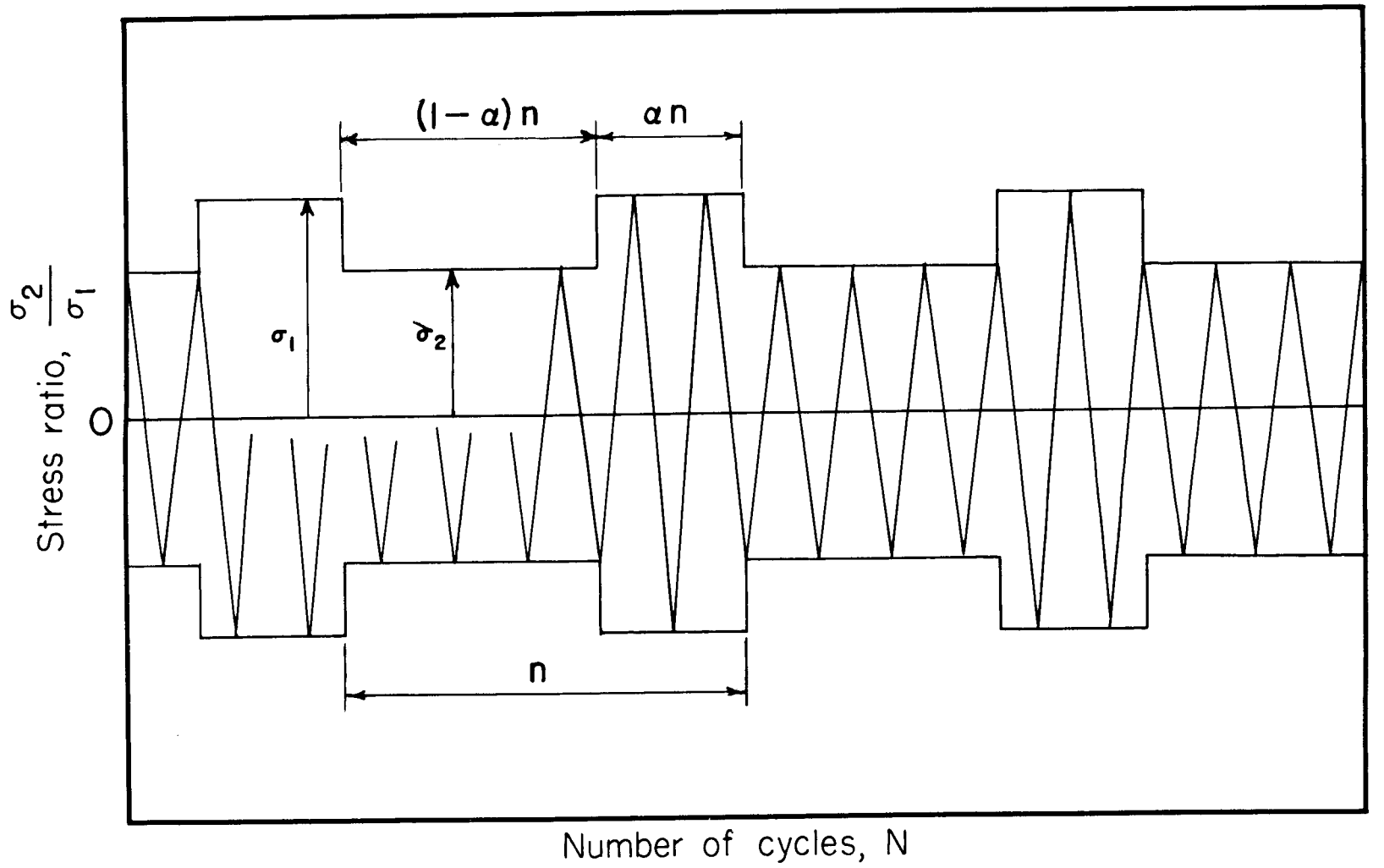

(a) Stress history of two-stress repeated block experiments.

Figure 4. - Stress histories.

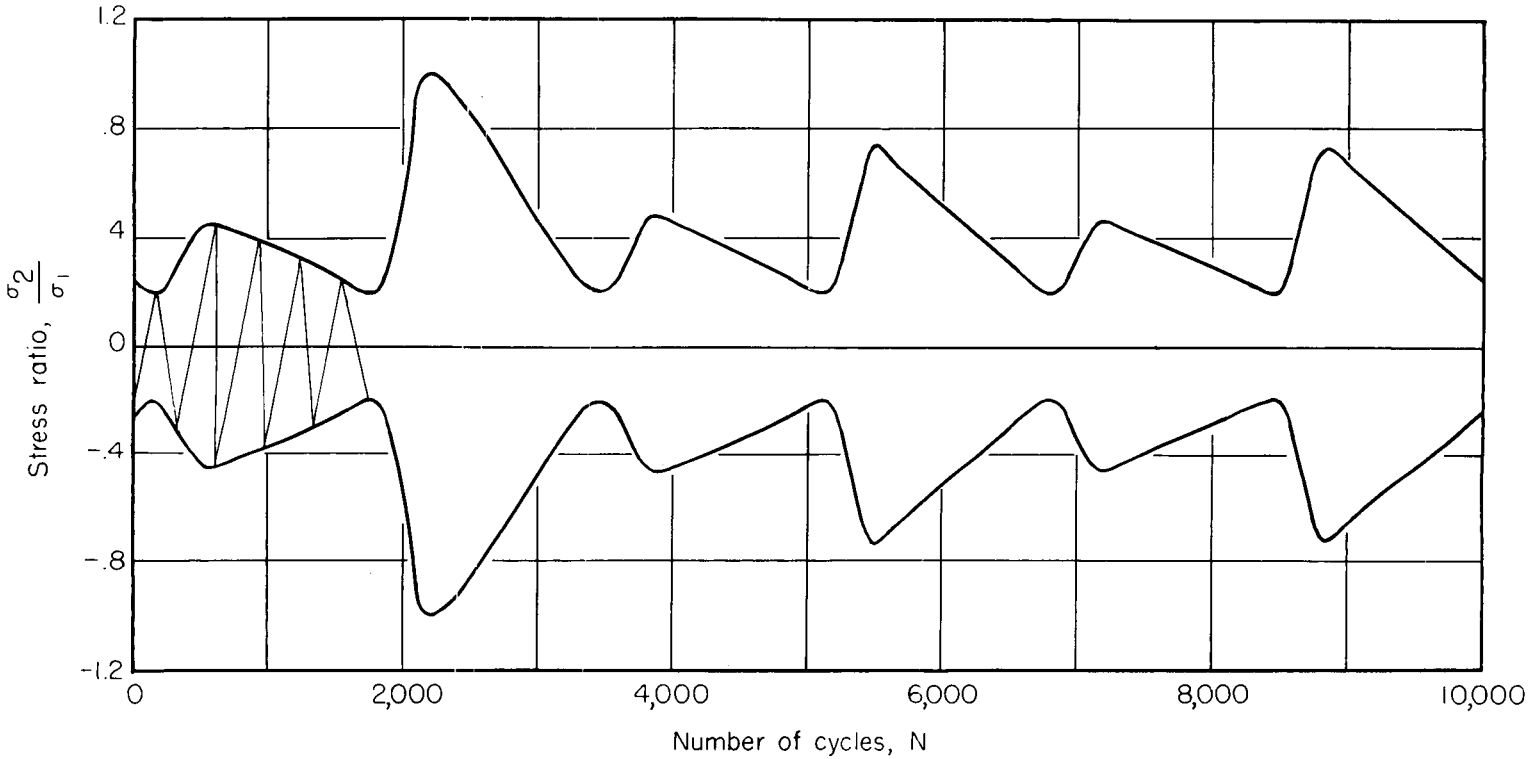

(b) Stress history of continuously varying stress experiment; 2024-T4 aluminum alloy; stress history 1.

Figure 4.- Concluded.

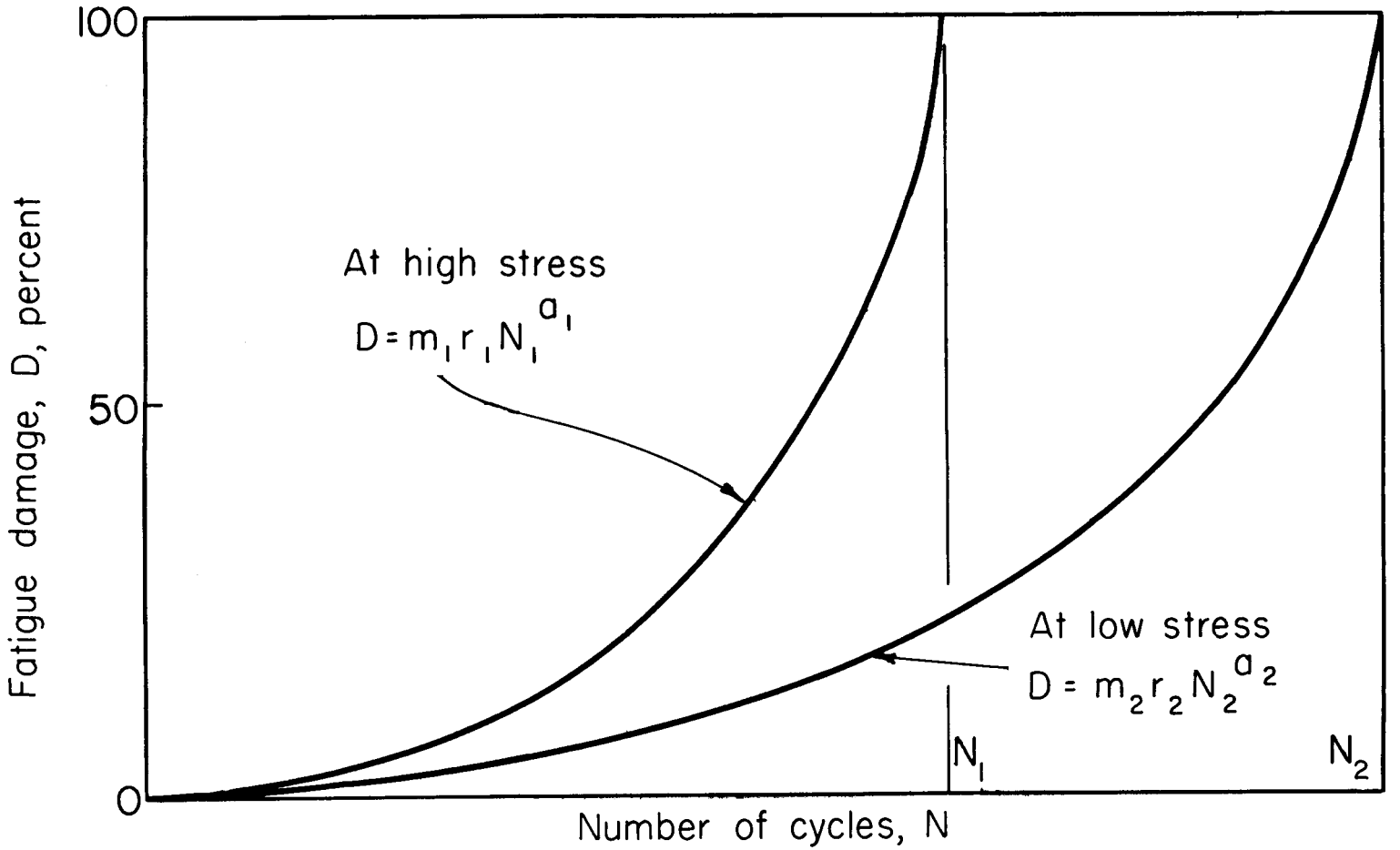

Figure 5. - Hypothesis of progress of fatigue damage caused by repetitions of stress.

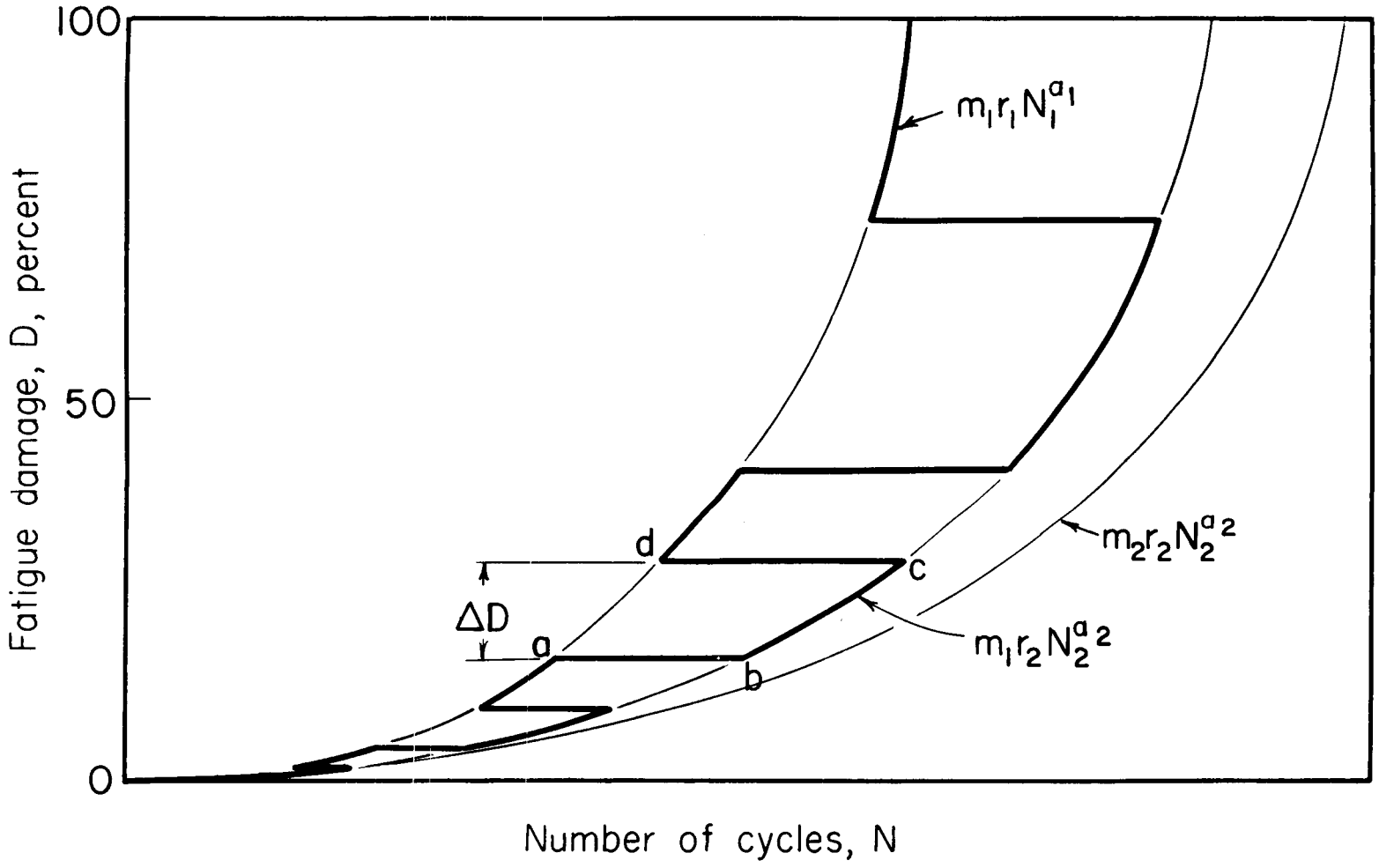

Figure 6.- Hypothesis of progress of fatigue damage during repeated block fluctuating stress-amplitude history. At high stress the number of damage nuclei formed is m_1. These damage nuclei are propagated at both high and low stresses.

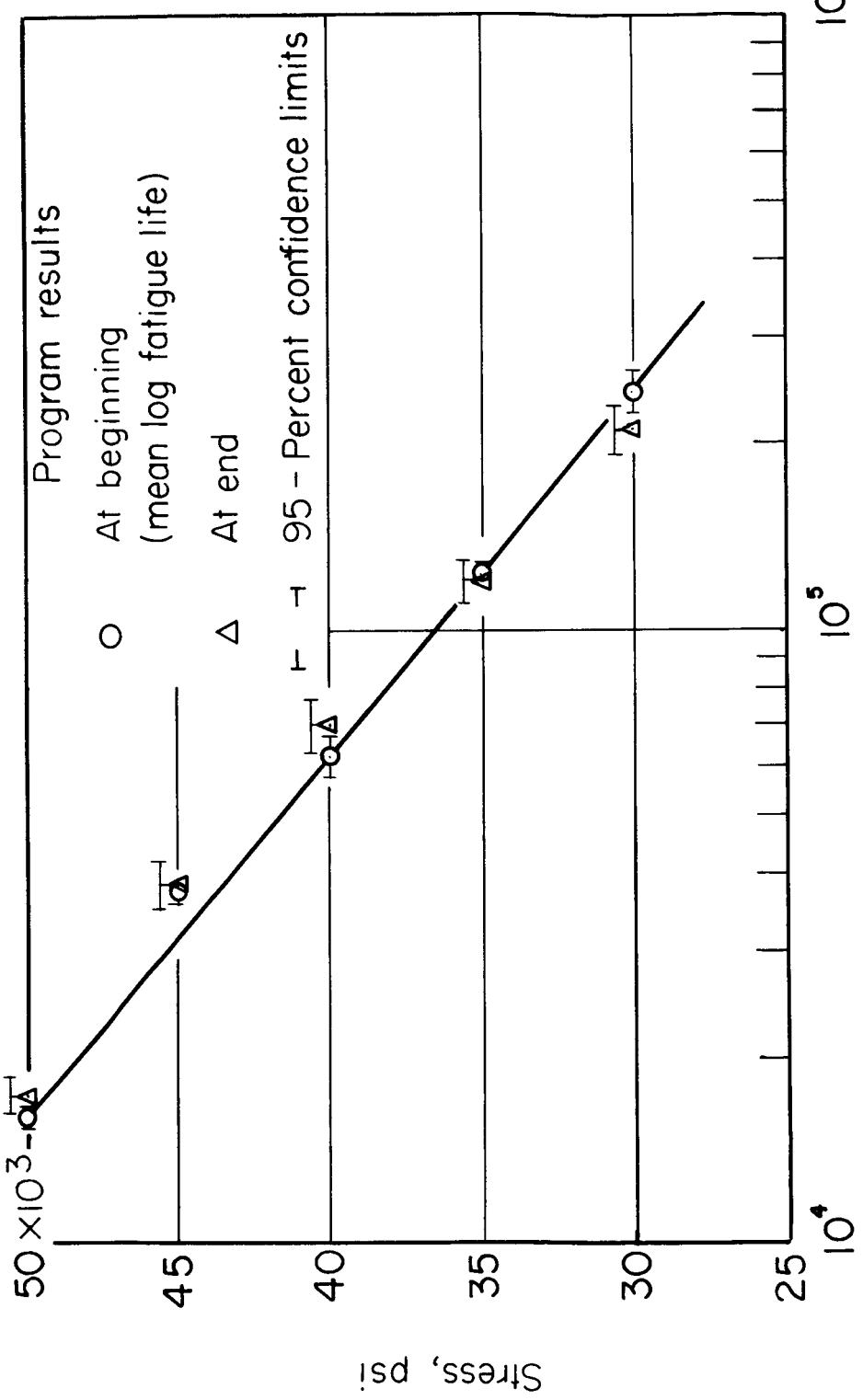

(a) 2024-T4 aluminum-alloy wire.

Figure 7.- Fatigue-data curves.

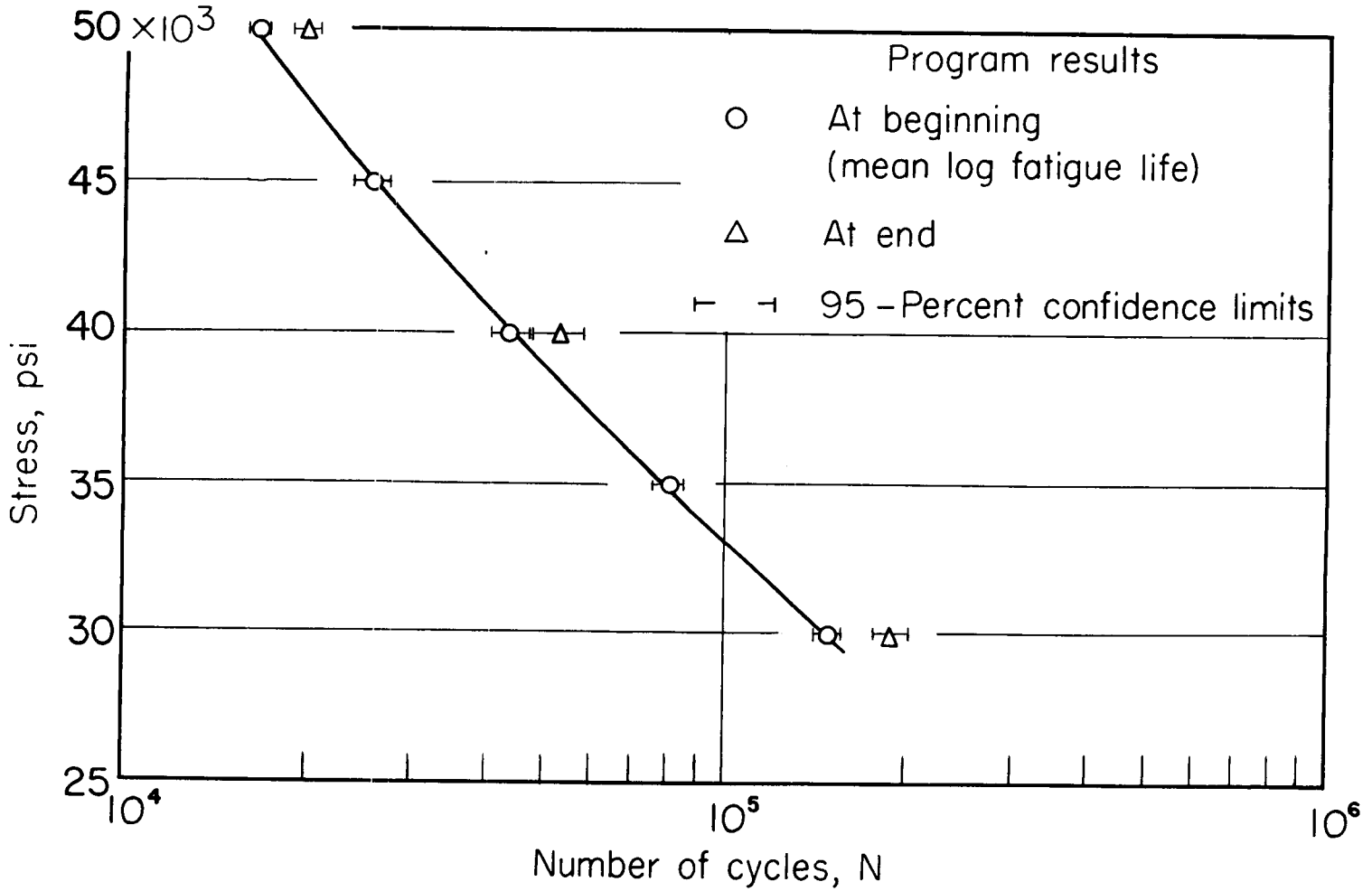

(b) 7075-T6 aluminum-alloy wire.

Figure 7.- Continued.

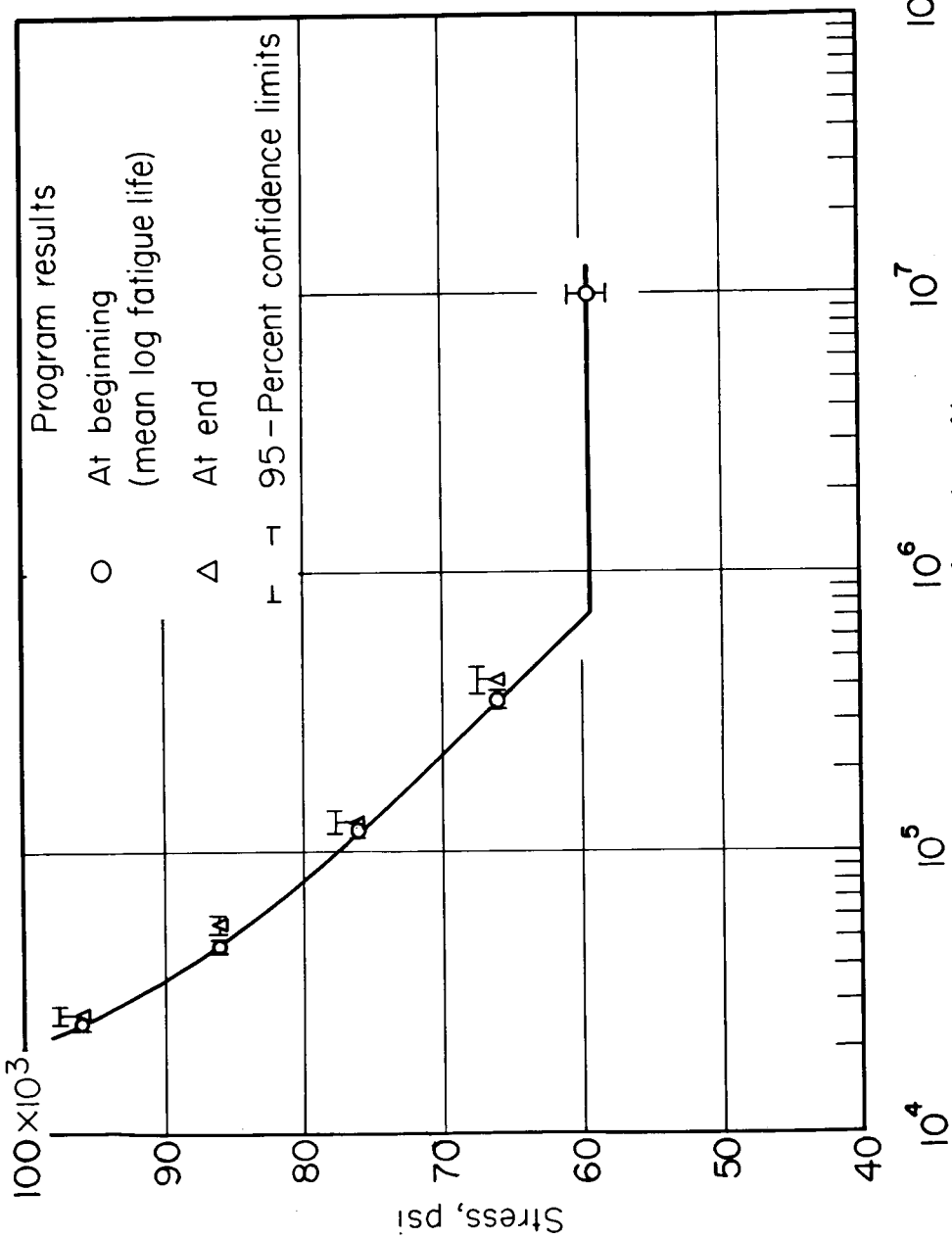

(c) Hard-drawn steel wire.

Figure 7.- Concluded.

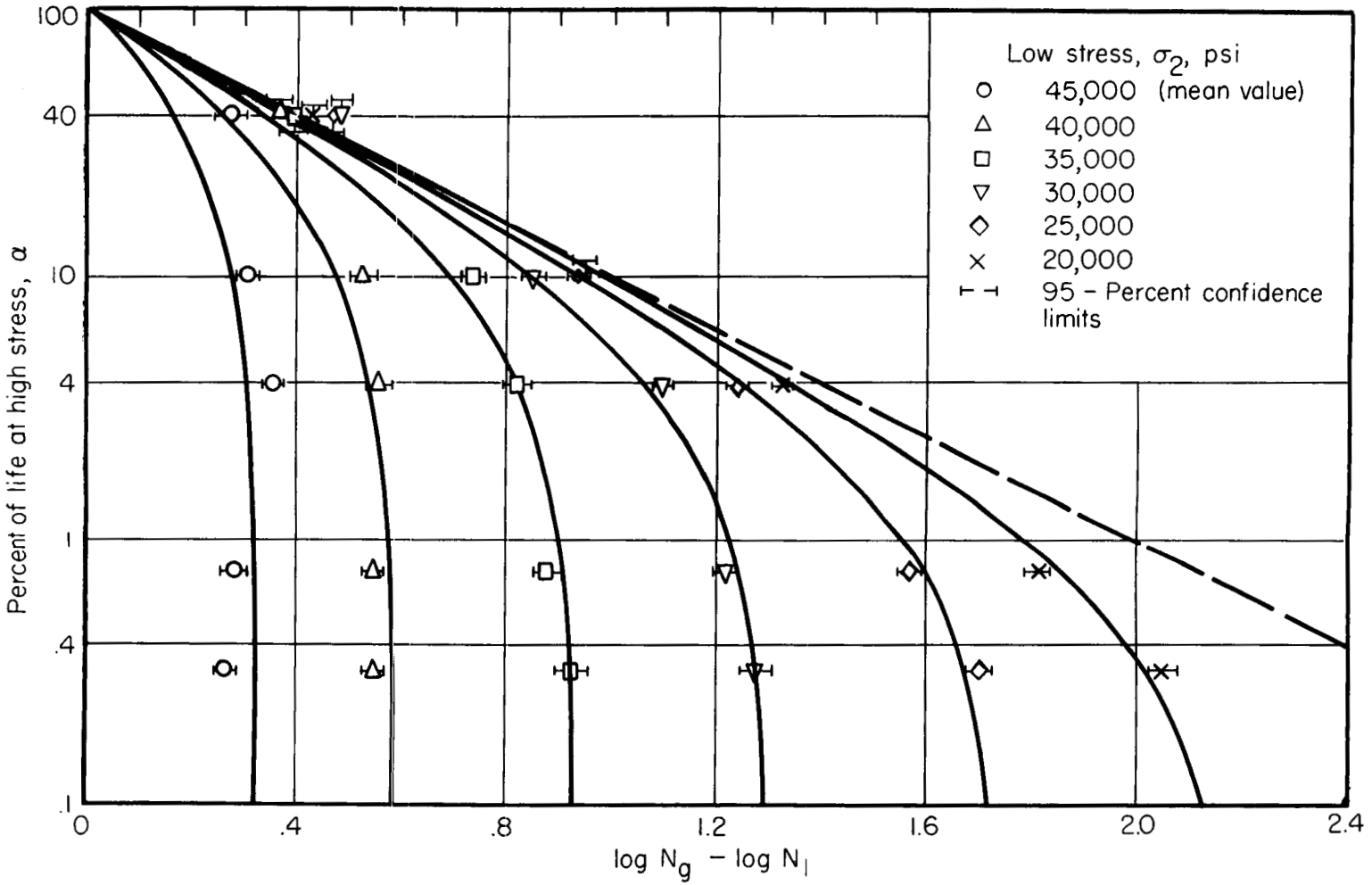

(a) High stress, 50,000 psi; 2024-T4 aluminum-alloy wire; machine 3.

Figure 8.- Data for two-stress repeated block experiments.

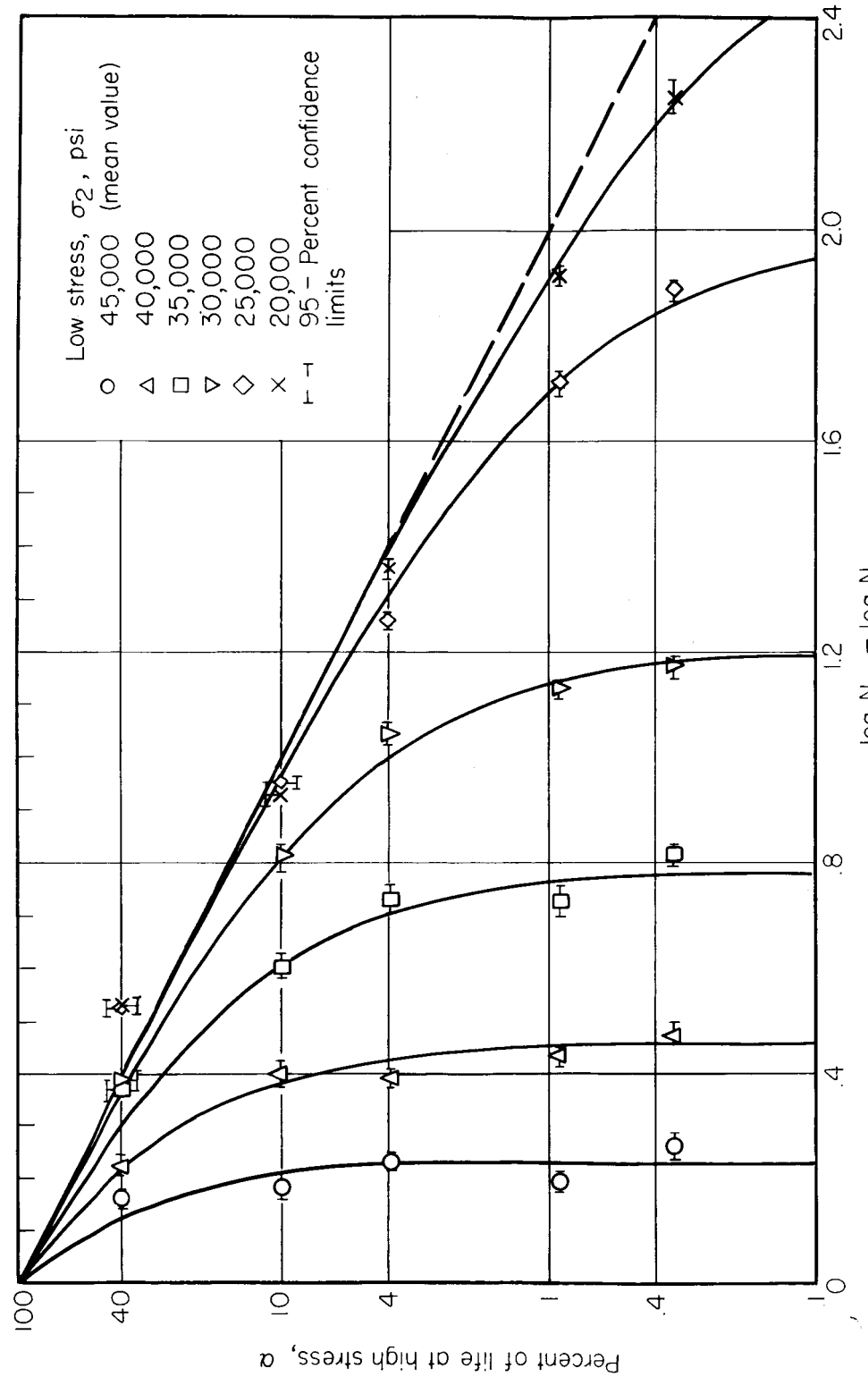

(b) High stress, 50,000 psi; 7075-T6 aluminum-alloy wire; machine 4.

Figure 8.- Continued.

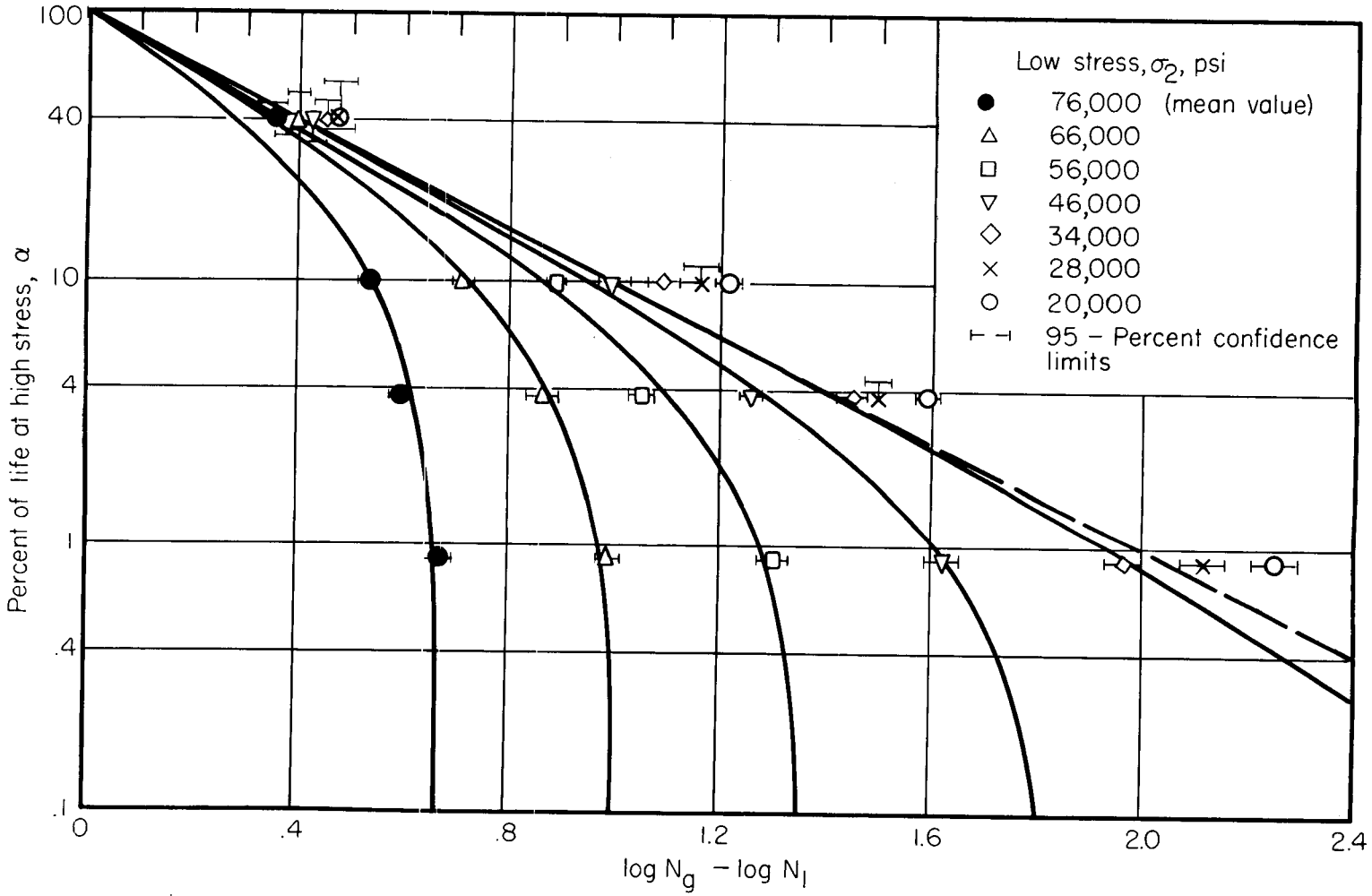

(c) High stress, 96,000 psi; hard-drawn steel; machine 5.

Figure 8.- Concluded.

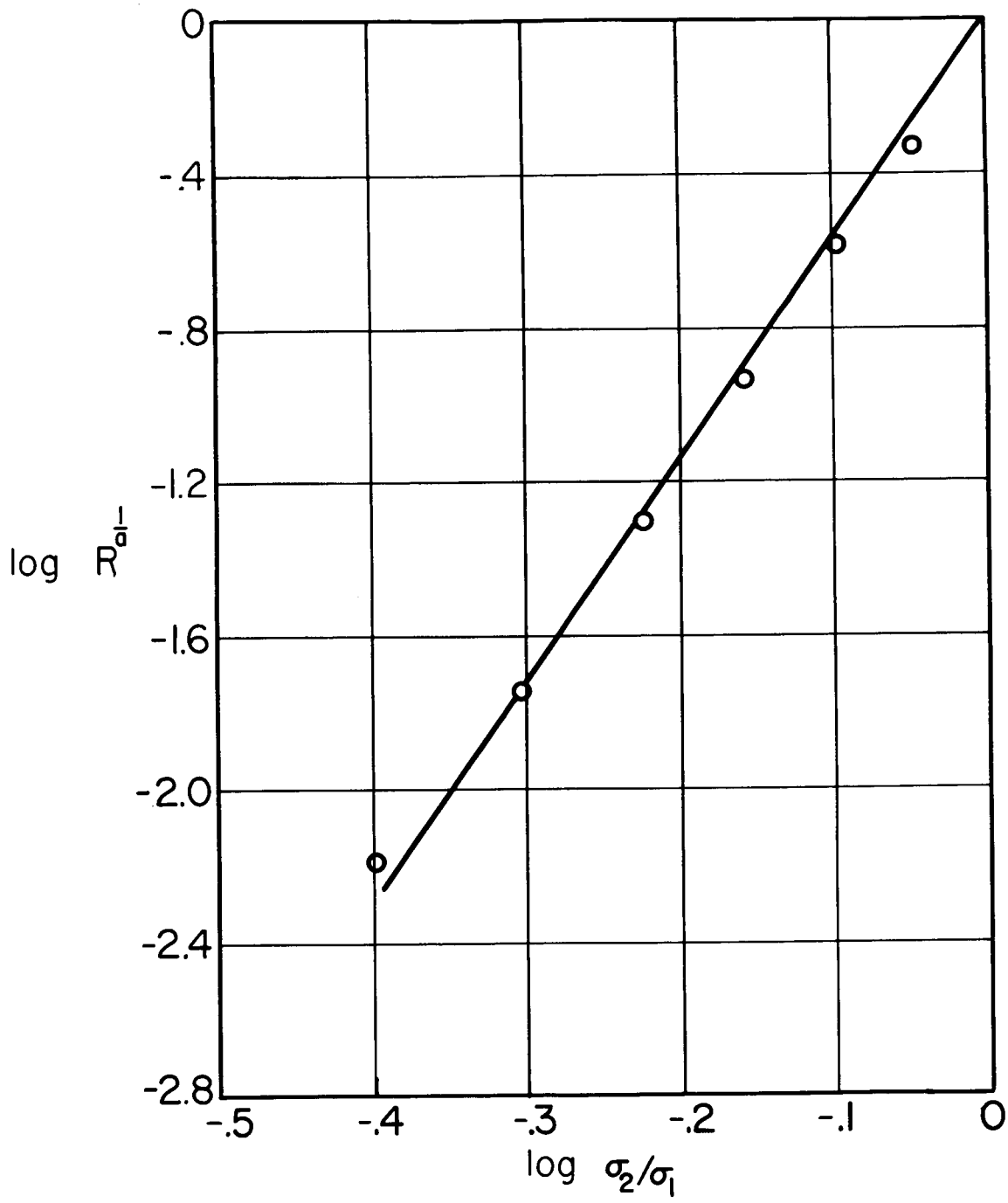

(a) 2024-T4 aluminum-alloy wire.

Figure 9.- Correlation between relative rates of damage propagation and amplitudes of imposed stresses.

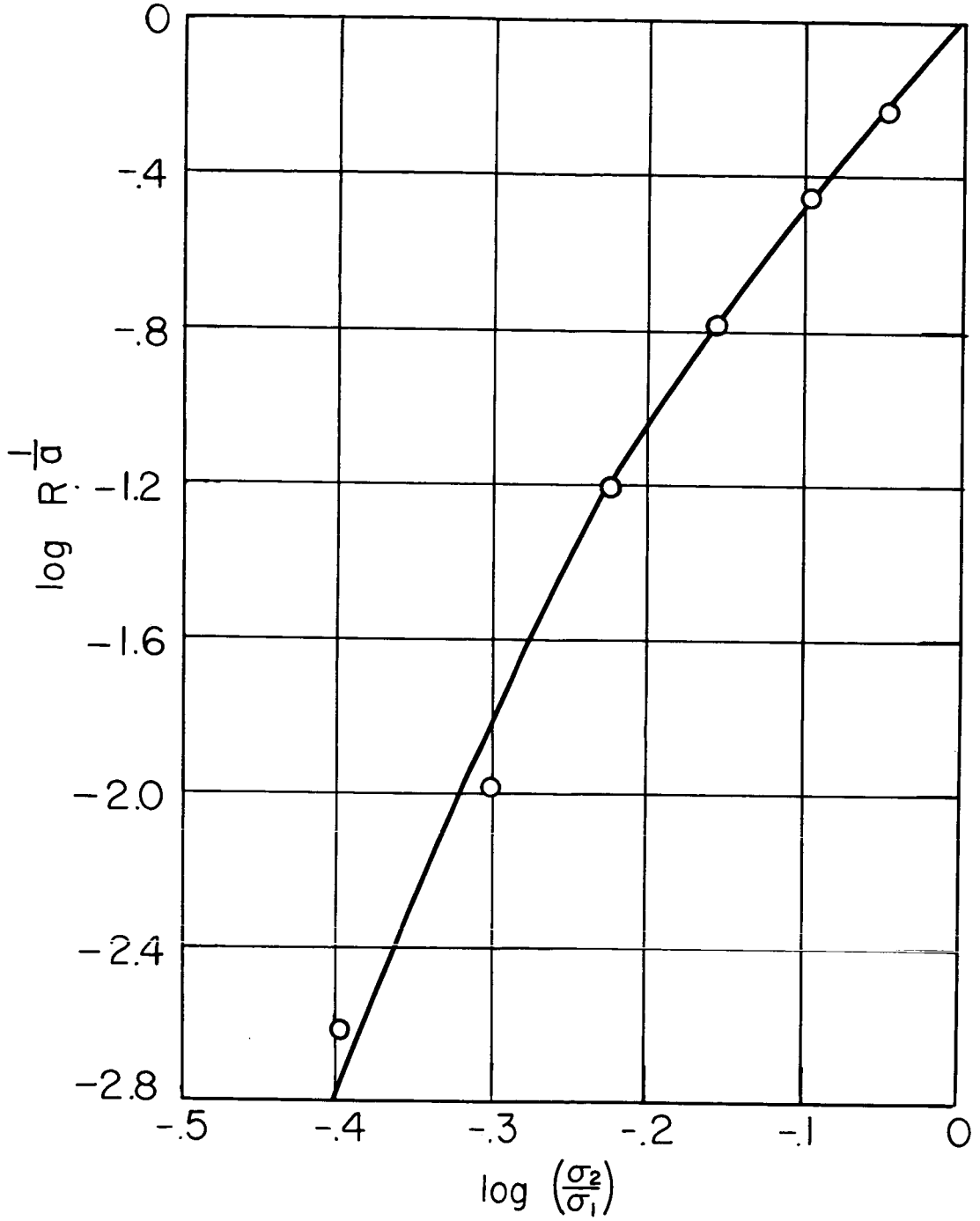

(b) 7075-T6 aluminum-alloy wire.

Figure 9.- Continued.

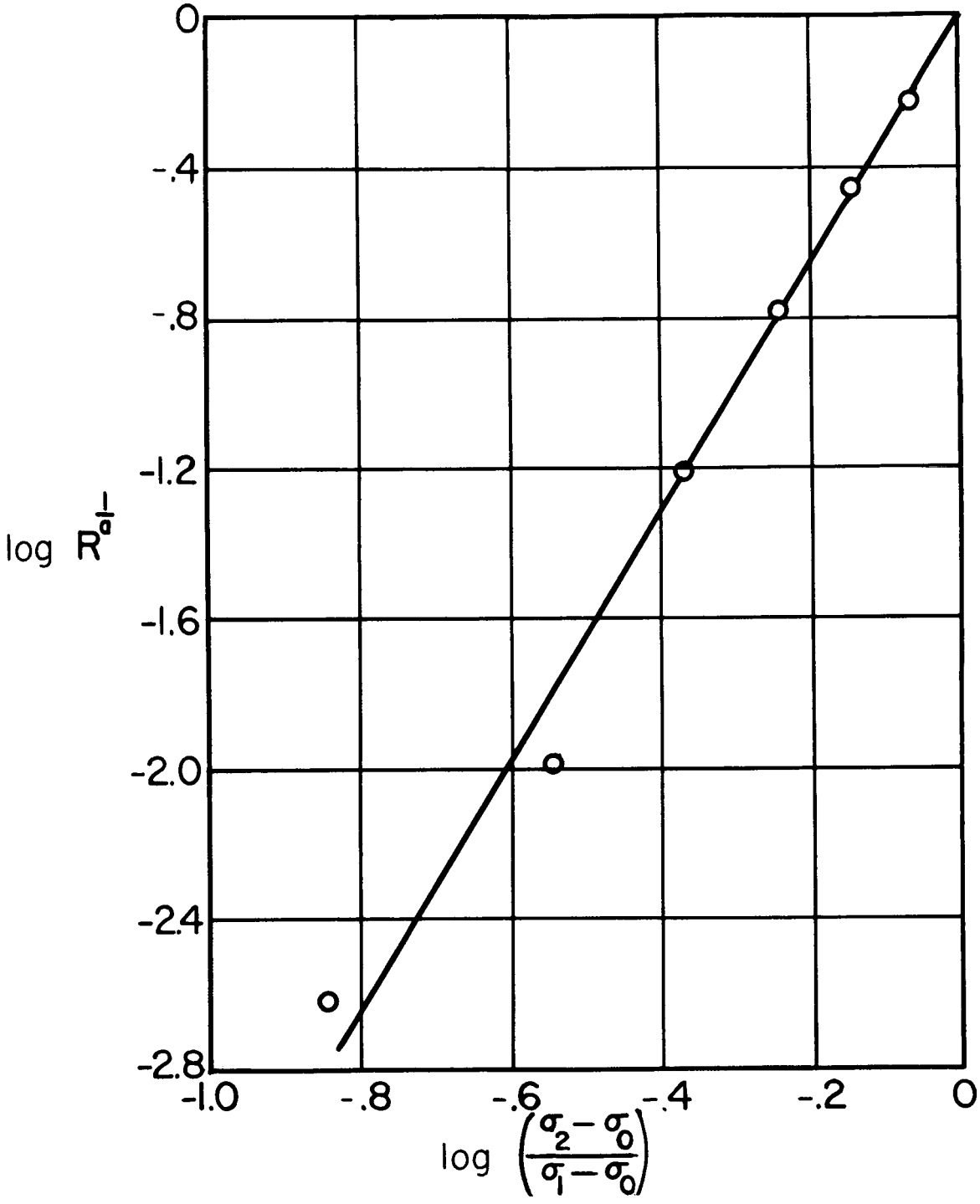

(c) 7075-T6 aluminum-alloy wire. σ_0 = 15,000 psi.

Figure 9. - Continued.

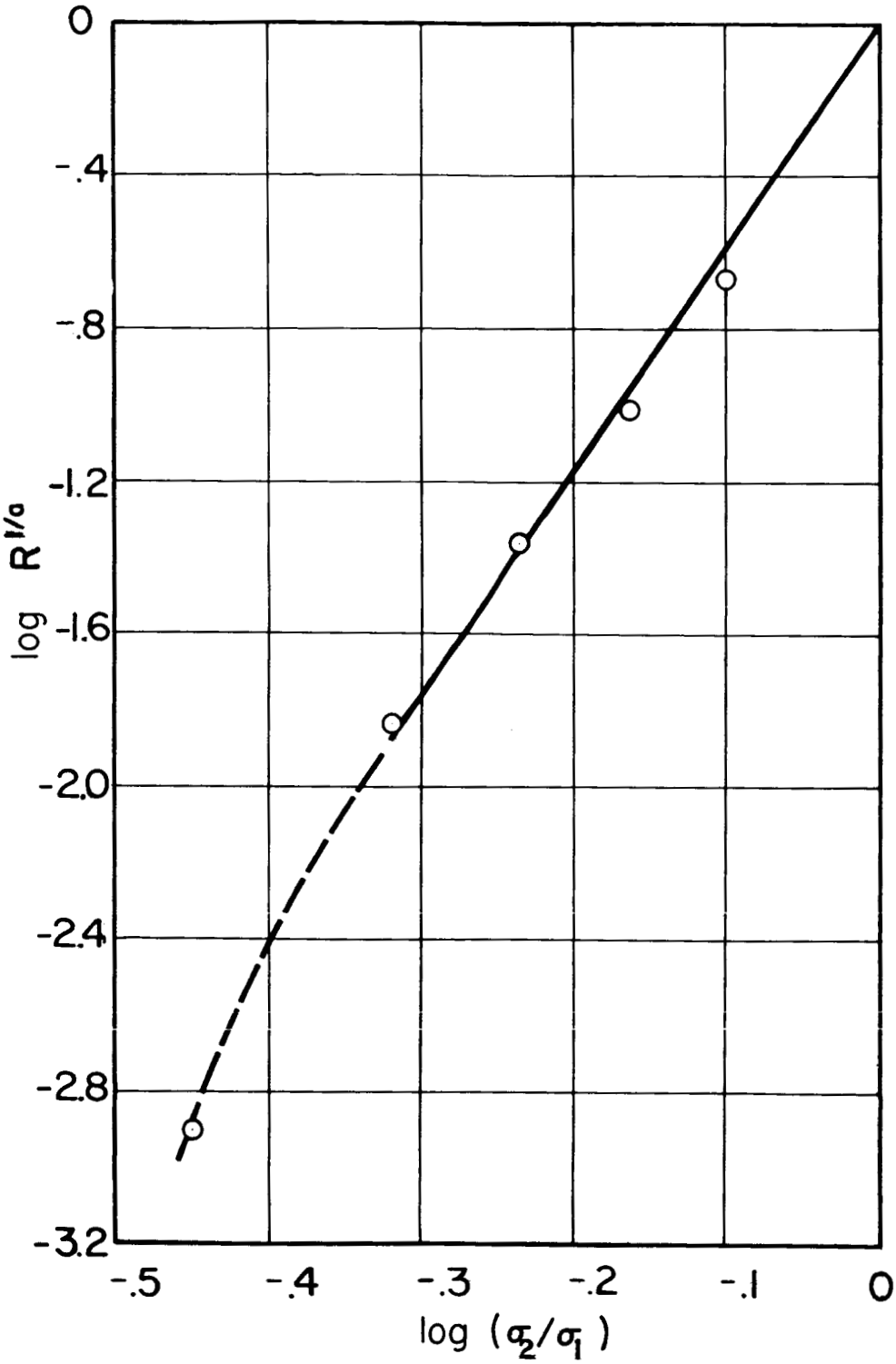

(d) Hard-drawn steel wire. Log $R^{1/a}$ against $\log(\sigma_2/\sigma_1)$.

Figure 9. - Continued.

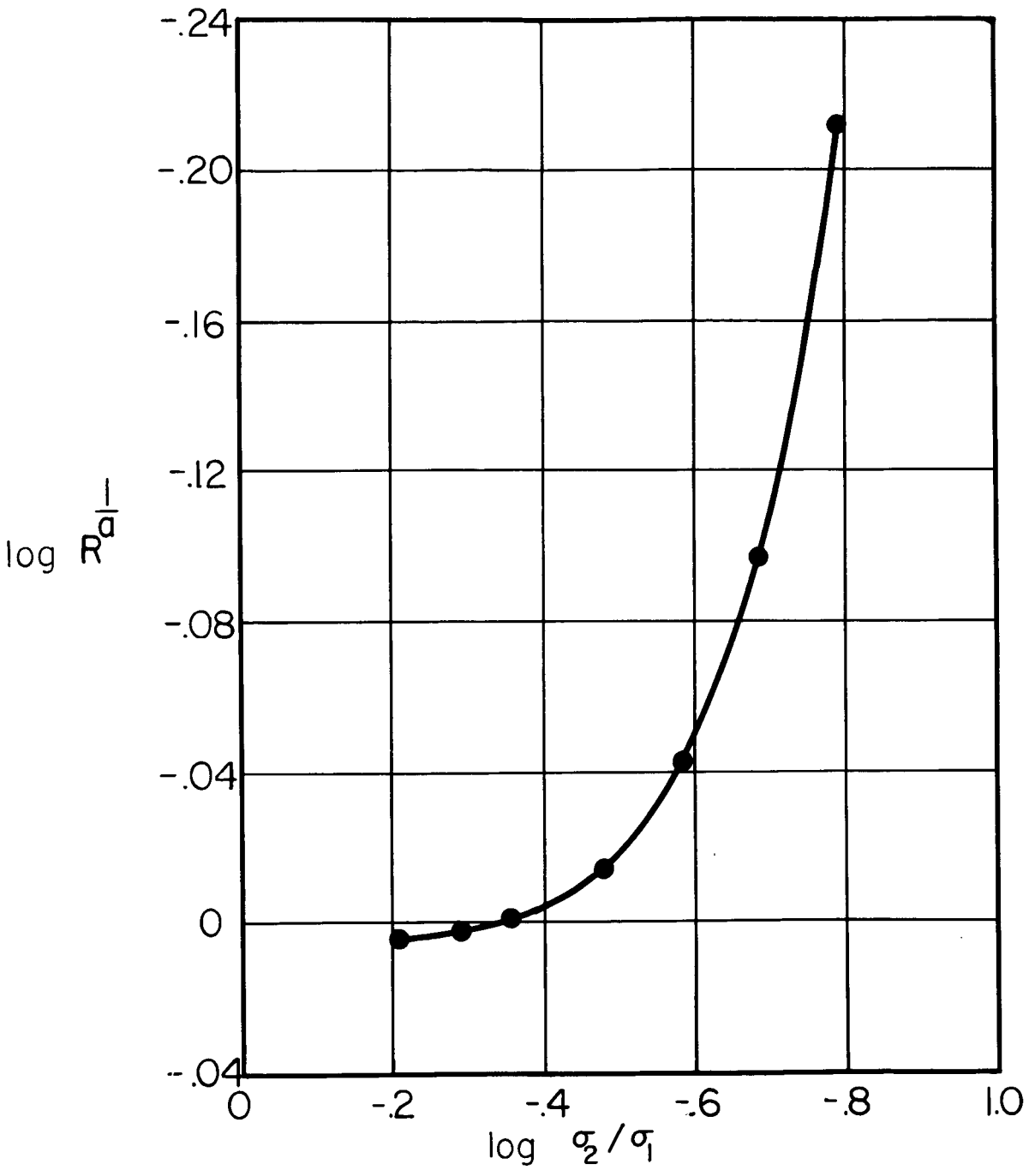

(e) Wires. $R^{1/a}$ against σ_2/σ_1.

Figure 9.- Concluded.

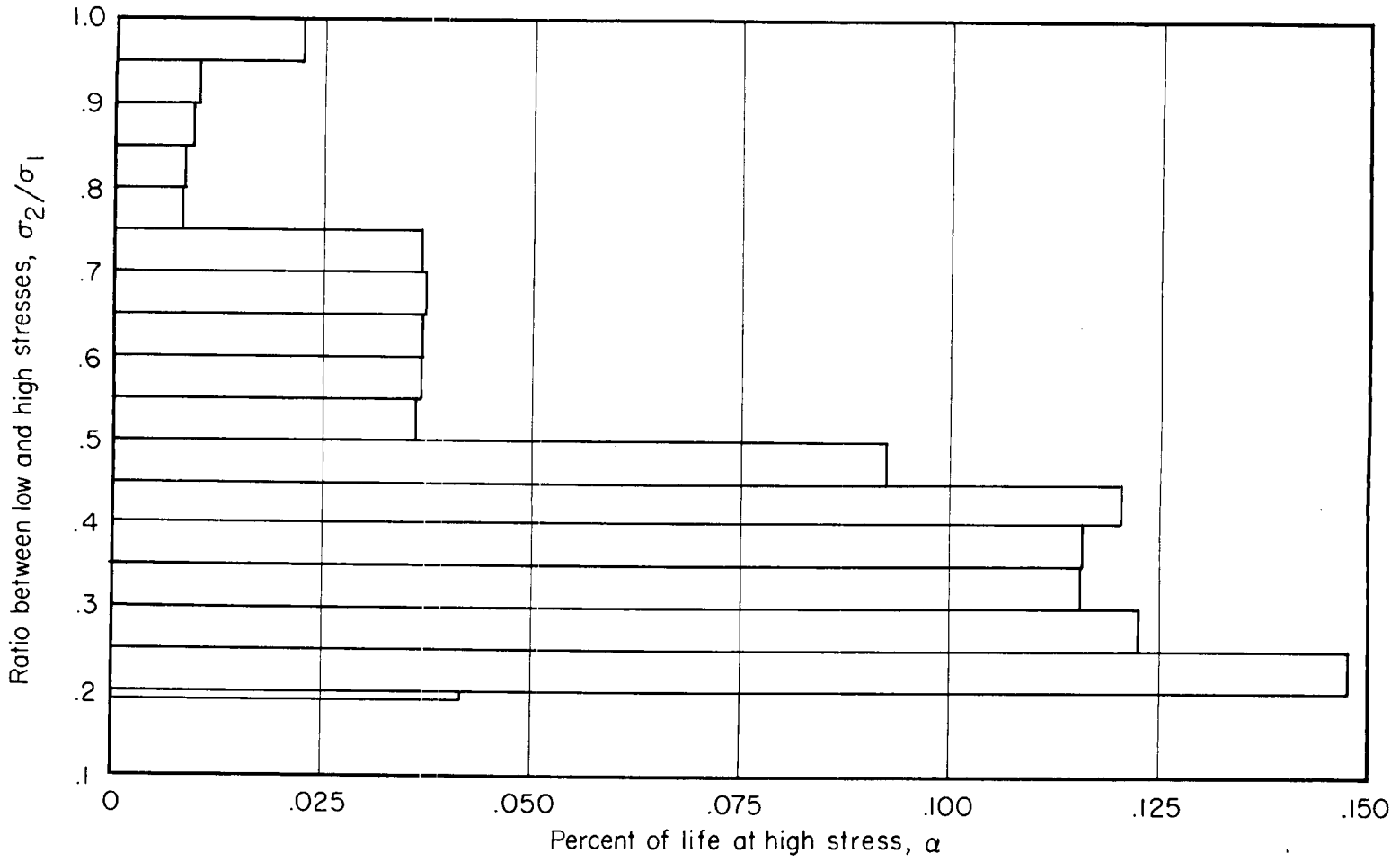

Figure 10.- Fraction of life at various stress levels for continuously varying stress experiment; stress history 1; 2024-T4 aluminum-alloy wire.

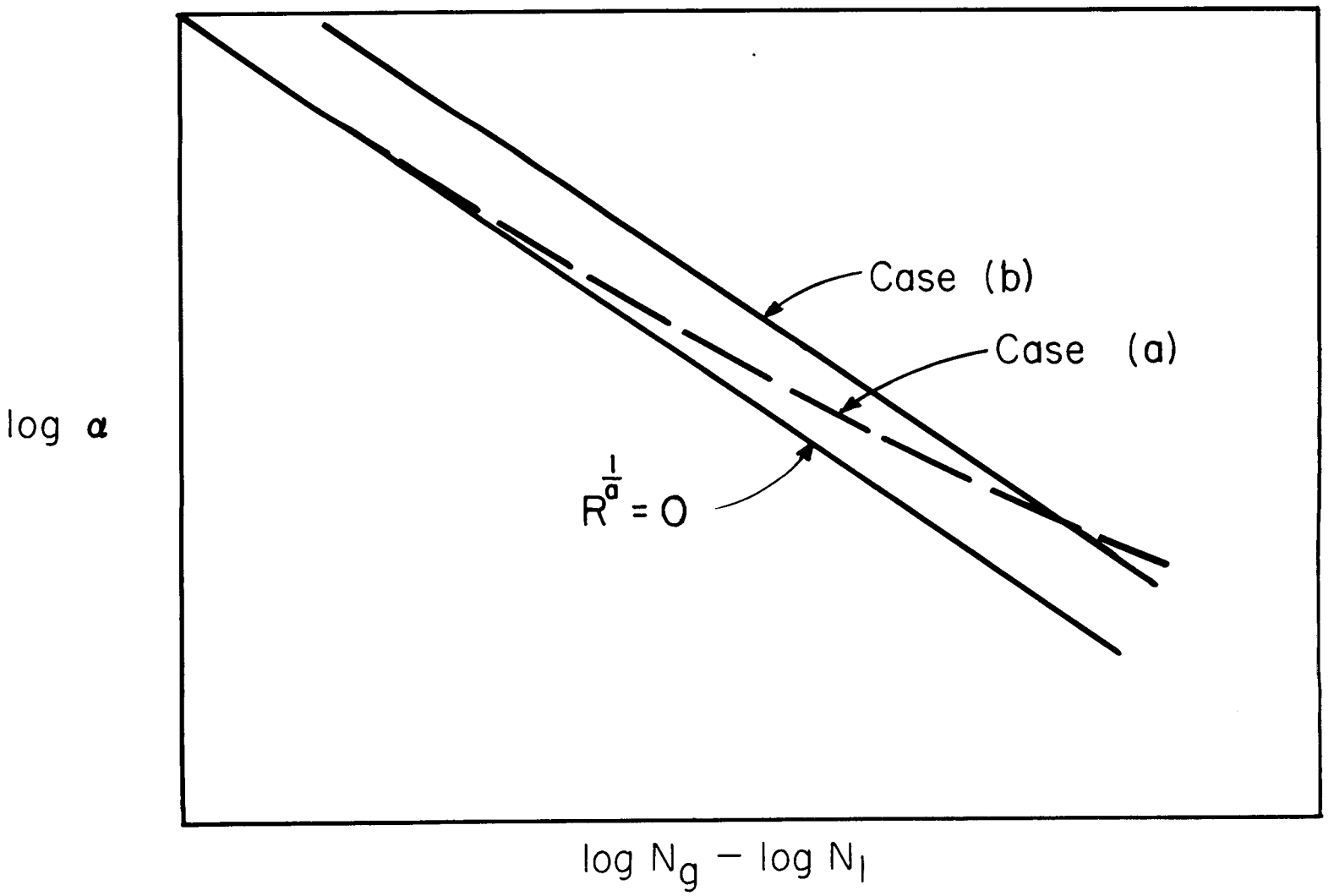

Figure 11.- Qualitative effect of strain aging on fatigue life for two-stress repeated block stress history.

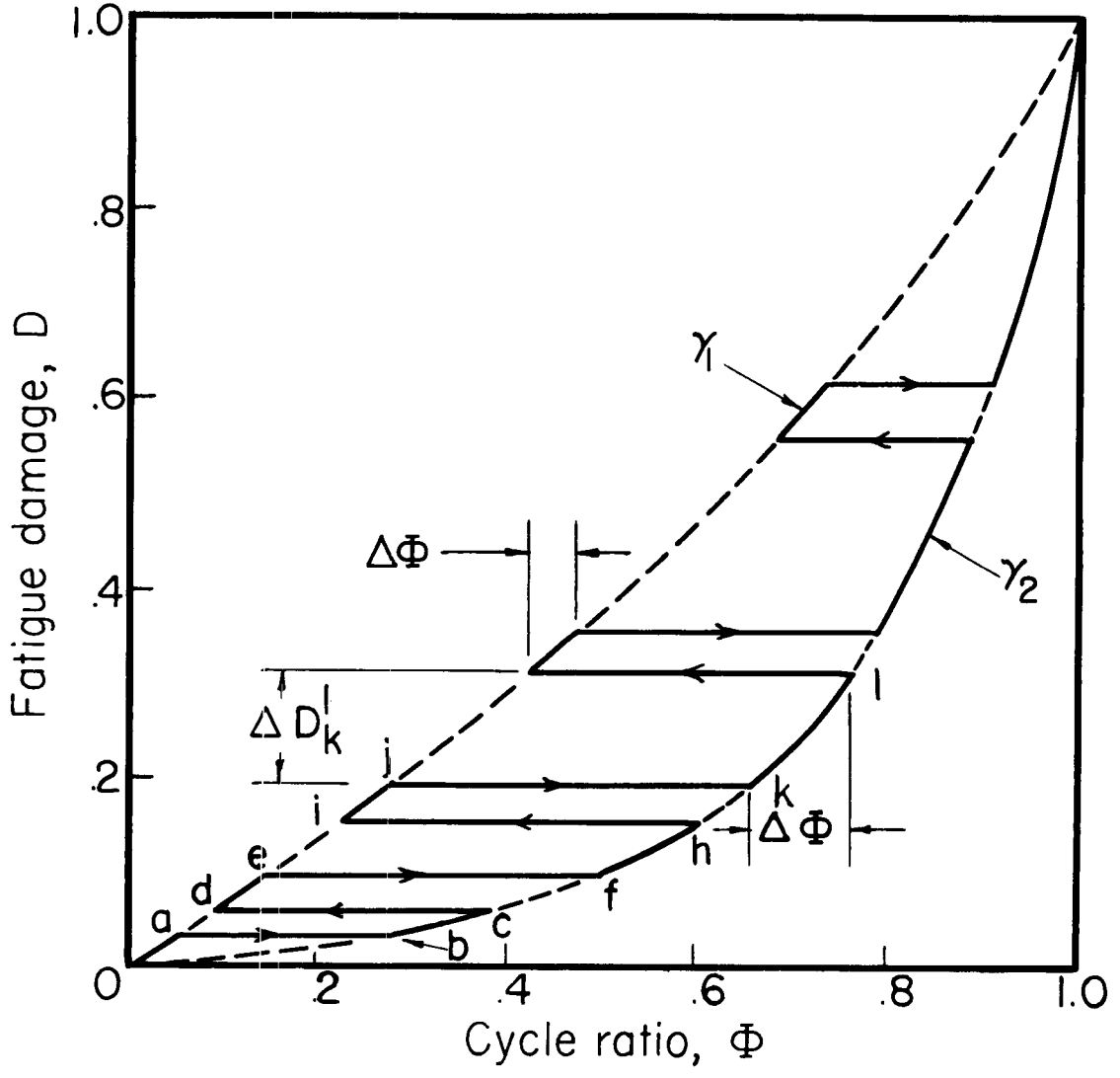

Figure 12.- Hypothesis of progress of fatigue damage in terms of cycle ratio for repeated block fluctuating stress amplitude history. $D = \Phi^{\gamma}$; $\gamma_2 > \gamma_1$.

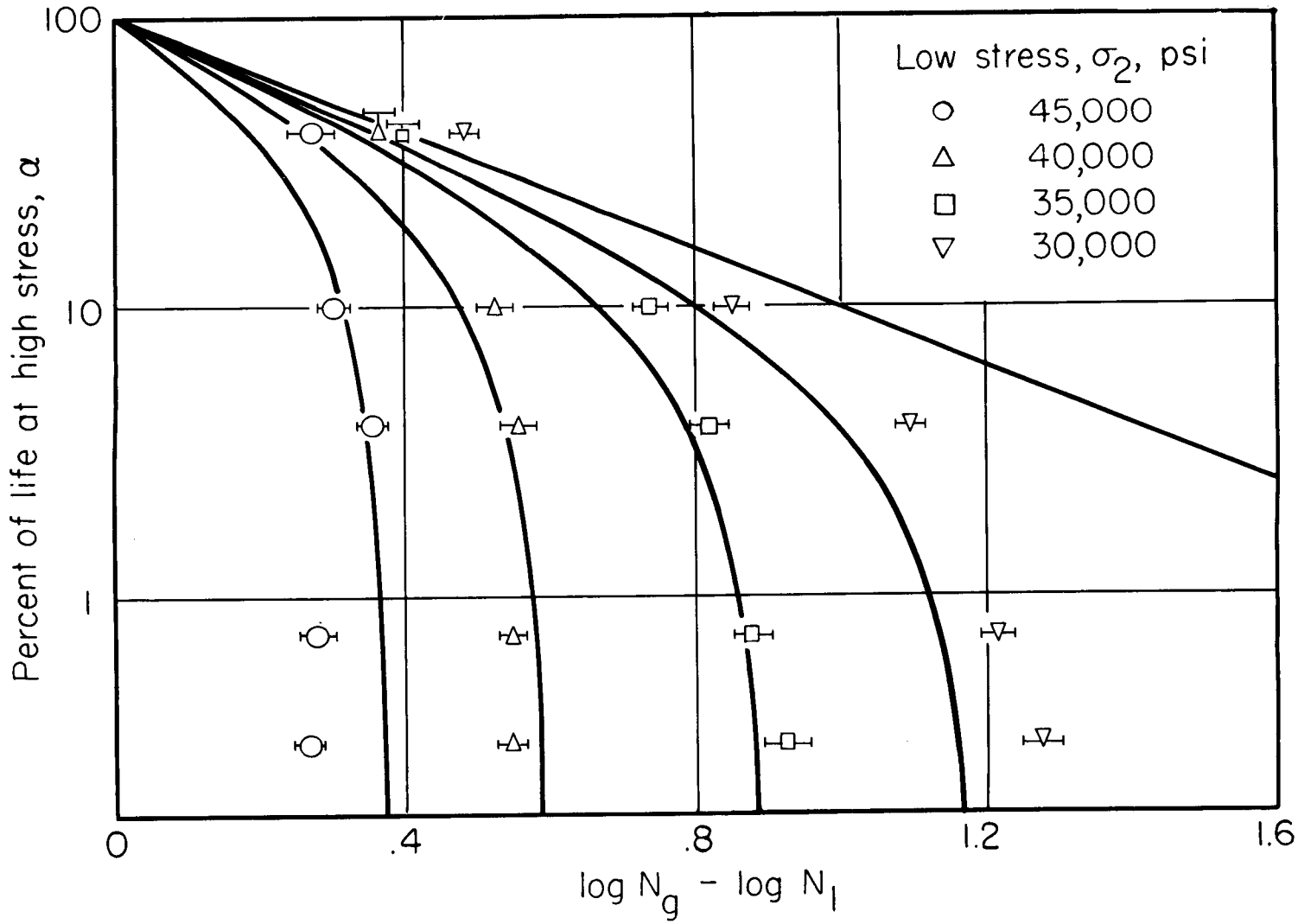

Figure 13.- Comparison of linear cumulative damage hypothesis (refs. 4, 5, and 6) with data for 2024-T4 aluminum-alloy wire; high stress, 50,000 psi.

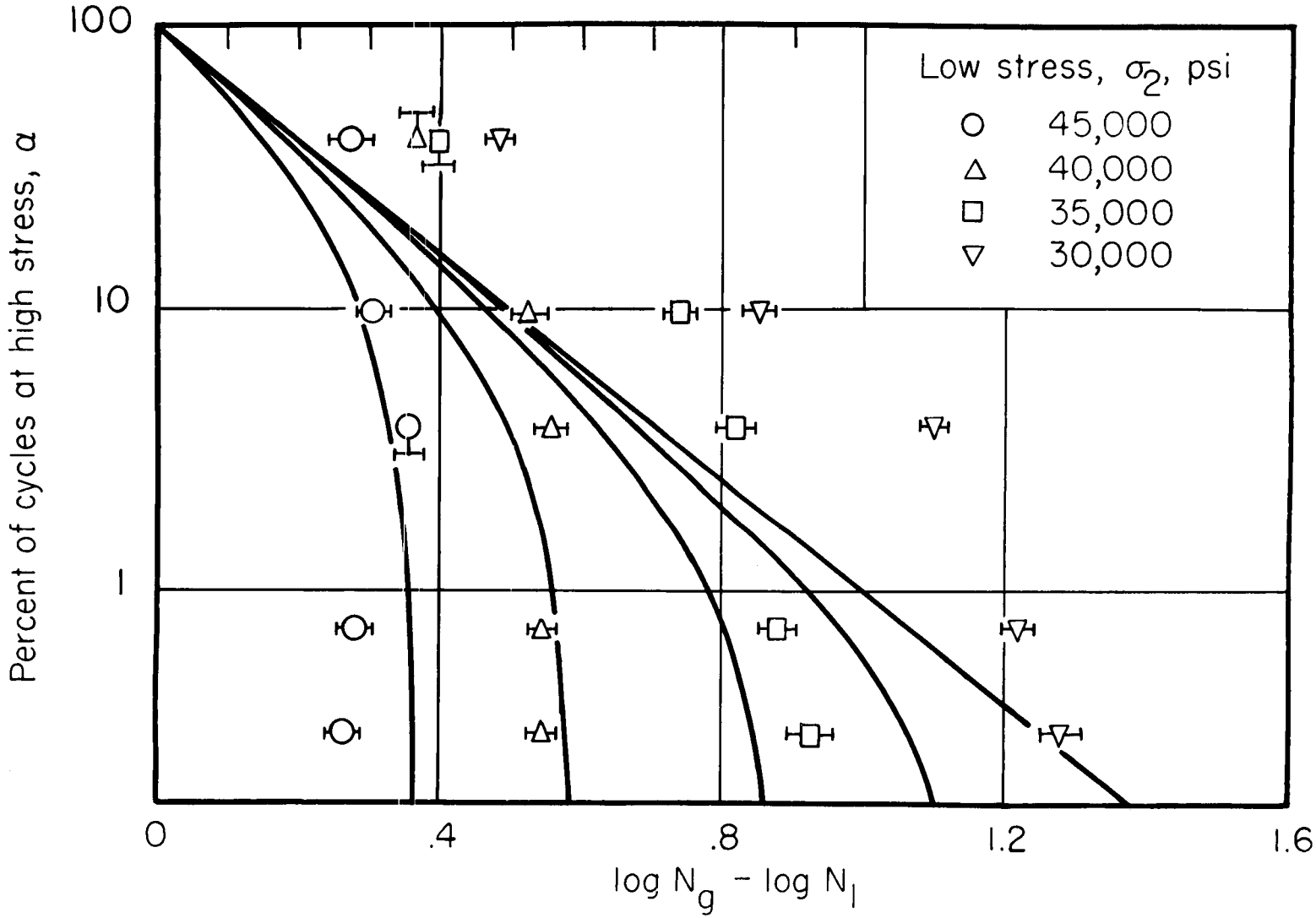

Figure 14.- Comparison of hypothesis of reference 8 with data for 2024-T4 aluminum-alloy wire; high stress, 50,000 psi.

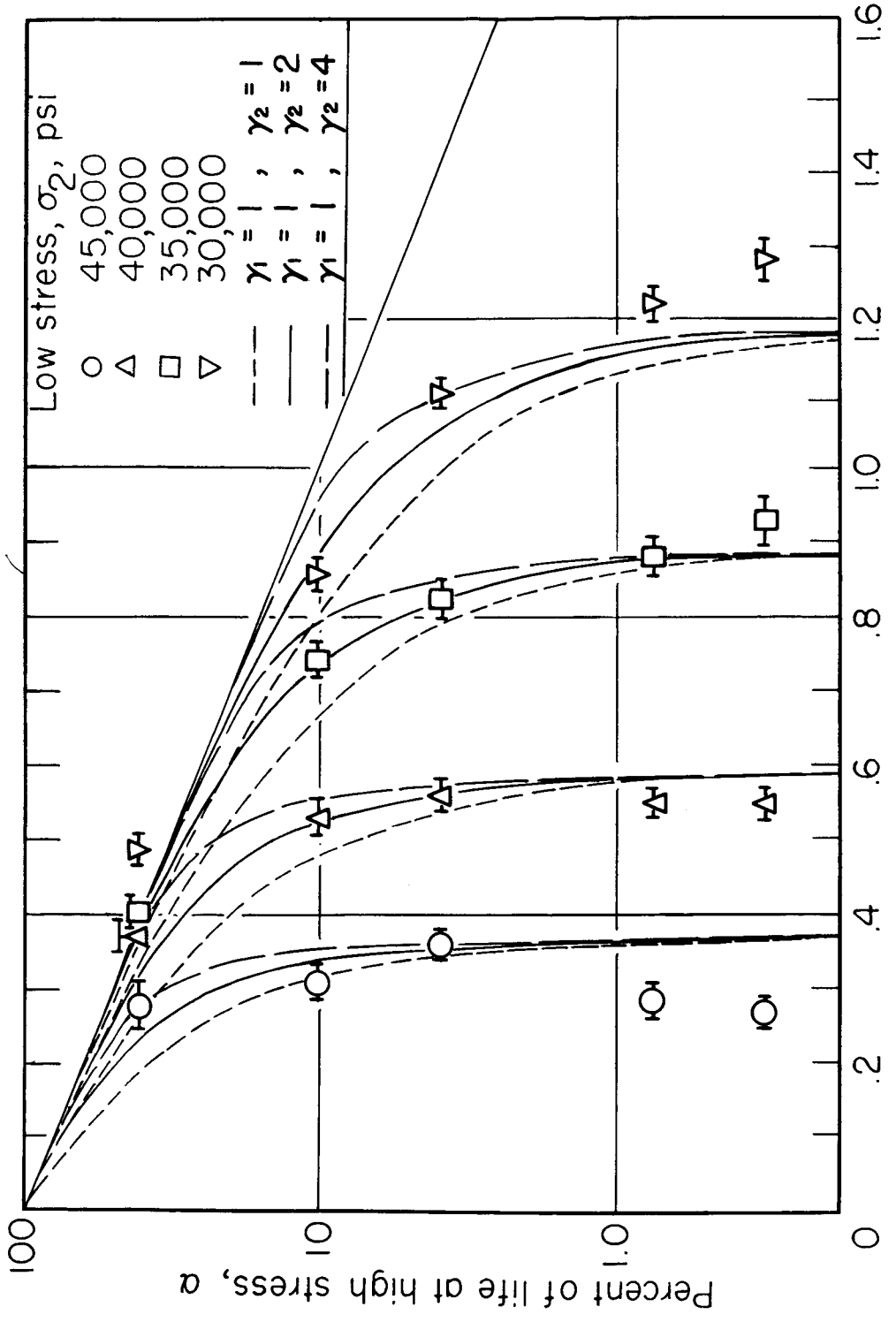

Figure 15.- Comparison of hypotheses of references 7 and 10 with data for 2024-T4 aluminum-alloy wire; high stress, 50,000 psi.